Past Precipitation, Watershed Characteristics, and Drought: Interactive Effects on Watersheds of Northern California

A Thesis
SUBMITTED TO THE FACULTY OF THE UNIVERSITY OF MINNESOTA BY

Erika Winner

IN PARTIAL FULFILLMENT OF THE REQUIREMENTS FOR THE DEGREE OF
MASTER OF WATER RESOURCES SCIENCE

Dr. Salli Dymond
April 2025

ACKNOWLEDGEMENTS

I would first like to thank Dr. Salli Dymond, your persistence is unmatched. Thank you for encouraging me to explore this field and doing your best to keep me on task. I know this has been a long path and I will be forever grateful that you gave me the time I needed to walk it.

Thank you to my committee members Dr. Joe Wagenbrenner and Dr. Byron Steinman for your ideas and feedback as I developed this project.

I would like to thank the United States Forest Service, the California Department of Forestry and Fire Protection, and the National Science Foundation (NSF-EAR-1807165) for funding my research. I would also like to thank CAL FIRE and USFS for providing me support in my fieldwork.

Liz Keppeler, thank you for sharing your life's work at Caspar Creek and helping shape relevant research questions for the watershed. Jayme Seehafer, your patience as I probed into what data was available and your work in getting me that data is greatly appreciated. To all of the US Forest Service folks that work at Caspar Creek, thank you for gathering the data that was foundational to this project.

I would like to thank Lynn Webb for answering my questions about forestry and timber harvest data. I would also like to acknowledge everyone at CAL FIRE Fort Bragg who provided support and collected the forestry data for this project.

Thank you to the University of Minnesota Duluth's Water Resources Science Program for the support and funding for me to present this work at the American Geophysical Union Fall Meeting. In particular, Tracy Fallon, without your regular checkins I could very easily have been lost to the advanced status doldrums, thank you for lighting the fire to get this thing done. To the Department of Earth and Environmental Science, thank you for providing a home and community on the UMD campus.

Yulia Petreshen, my field partner and perennial writing buddy, thank you for dragging me to the café every weekend to make sure I kept up with the progress, I owe you a million little treats. Shannon Christiansen, it's been a long and bumpy road, I'm so glad I've had you by my side to share in both tears and laughter. We have both worked so hard, I can't wait to cross the finish line with you. To all of my friends and colleagues, your encouragement and empathy has meant the world to me. I will be forever grateful.

Edwin Diaz, the guy I found in the woods, you are perhaps my greatest distraction, but my biggest cheerleader. Thank you for the patience and the pushes.

Finally, I would like to thank my family. Mom, thank you for teaching me to read water and work with the flow. Dad, thank you for always keeping me open to new ideas and possibilities. Tyson, thank you for being my stick in the water, showing me the way. I am so thankful that this family is my family.

ABSTRACT

Forested watersheds in Western North America are experiencing more frequent drought due to climate change, which impacts drinking water resources and stresses vulnerable aquatic species. Watershed properties, such as aspect, elevation, soil type, vegetation composition, and stand age, are known to impact runoff through differences in evapotranspiration and storage. Drought may further change the hydrological function, or precipitation-runoff relationship of a watershed. In this study, I investigated how watershed properties provide resilience against drought in forested watersheds. Precipitation and streamflow data from twelve sub-watersheds in the Caspar Creek Experimental Watersheds (California, USA) were collected from 2001-2017. Sub-watershed mean aspect, mean stand density index, and maximum soil depth correlated significantly with annual runoff ratios. To assess the hydrological functioning of sub-watersheds at different timescales, streamflow and runoff ratios were correlated to lags of past precipitation at annual, seasonal, and monthly timescales. Past precipitation was found to be an insignificant driver of streamflow or runoff ratios at annual and seasonal timescales, and significant for streamflow up to three months. These results may help in understanding the drivers of watershed resilience to aid in adaptive land management decisions.

Table of Contents

LIST OF TABLES

LIST OF FIGURES

LIST OF ABBREVIATIONS

Abbreviation	**Definition**
AIC	Akaike Information Criterion
ANOVA	Analysis of Variance
BA	Basal Area
CAL FIRE	California Department of Forestry and Fire Protection
CCEW	Caspar Creek Experimental Watersheds
DBH	Diameter at Breast Height
DEM	Digital Elevation Model
ESRI	Environmental Systems Research Institute, Inc.
ET	Evapotranspiration
GIS	Geographic Information System
Ha	Hectare
HSD	Tukey Honest Significant Difference
HY	Hydrologic Year
JDSF	Jackson Demonstration State Forest
LiDAR	Light Detection and Ranging
NF	North Fork Caspar Creek
NRCS	National Resource Conservation Service
P	Precipitation
PET	Potential Evapotranspiration
PRISM	Parameter-elevation Relationships on Independent Slopes Model
PSW	Pacific Southwest Research Station
Q	Streamflow
r_p	Pearson lag-correlation coefficient
RR	Runoff Ratio
$\overline{RRm}$	Modified Average Monthly Runoff Ratio
S	Storage
SD	Standard Deviation
SDI	Stand Density Index
SF	South Fork Caspar Creek
SPI	Standardized Precipitation Index
TWI	Topographic Wetness Index
USDA	United States Department of Agriculture
WY	Water Yield

1. INTRODUCTION

Across the Pacific Northwest, home to some of the world's most productive forests, climate change is causing warming temperatures and shifts in regional precipitation patterns (Asarian and Walker, 2016; Seager et al., 2017; Swain et al., 2014; Williams et al., 2015). These shifts include more extreme and frequent drought. Droughts can lead to drinking water shortages, warming stream habitats, and forest stand die-offs (Bogan et al., 2019; Deitch et al., 2018; Dong et al., 2019). Hydrological resilience, or the ability of a catchment to absorb change and maintain or quickly regain hydrologic function, is at question in the face of a changing climate (Gerten et al., 2005) — what will determine the future resilience of these forested watersheds and how will their functioning change? Studying the rainfall-runoff relationship and the properties of watersheds which impact their functioning may serve to answer this question.

The coastal Pacific Northwest has a Mediterranean climate, with wet winters and dry summers, which creates a perennial challenge: the times with the most water availability are opposite those with the most energy availability. This asynchrony has consequences on how water moves through watersheds, as it falls as precipitation, evaporates off surfaces, is taken up and transpired by plants, stored in soil or groundwater, and runs off into streamflow. Over the summer, streams may run dry without precipitation inputs, however, adequate watershed storage can allow streams to retain baseflow through long dry periods (Aulenbach and Peters, 2018; Coble et al., 2020; Moges et al., 2022). Given the challenges of estimating watershed storage, we can look at past precipitation to determine the resilience of streamflow in a watershed. A particularly wet season could allow a watershed to retain streamflow through the dry season (Keppeler et al., 2024; Nippgen et al., 2016). Following this logic, a wet year might carry over into a drought, providing sufficient streamflow despite below average precipitation. The question remains—at what timescales (e.g., annual, seasonal, or monthly) does past precipitation affect present streamflow?

Beyond past precipitation, biophysical characteristics of a watershed, such as elevation, geology, or forest composition, have been shown to significantly control the relationship between precipitation and streamflow (Coble et al., 2020; Creed et al., 2014; Jones et al., 2012; Moges et al., 2022; Nippgen et al., 2016; Saft et al., 2015; Segura et al., 2019). However, understanding to what degree these biophysical characteristics influence streamflow is still an area of active research. This knowledge gap can pose a challenge in assessing the significance of watershed studies, since despite the presence of replicates, the inherent variability derived from topography, geology, soils, and vegetation may confound study treatments (McDonnell et al., 2018; Wagenbrenner, 2018). For example, an analysis of watersheds across the United States found that while the average annual number of days of measurable precipitation was the strongest determinant of annual runoff ratio and coefficients of variance, topographic and geologic variables also had a significant impact (Chang et al., 2014). Nippgen et al. (2016) found that elevation and forest type were stronger controls on runoff ratios than watershed aspect. Furthermore, management activities such as forest harvesting and thinning can lead to changes in evapotranspiration, water yield, and water storage (Perry and Jones, 2016; Sun et al., 2015). The legacy effects of management may last for decades, however study results are mixed and the post-harvest activities are generally found to determine the extent of harvest effects on streamflow (Carr et al., 2014; Segura et al., 2020; Ziemer et al., 1996). While there is general agreement that biophysical characteristics impact the hydrologic function of watersheds, which characteristics serve as the dominant controls appears to be unique to each system.

Exogenous influences, such as drought, can generate dramatic disturbances to a watershed's function. Drought in the western United States is becoming increasingly common. In much of California, drought conditions are becoming the "new normal" due to anthropogenic-driven climate change as well as natural climate cycles (Seager et al., 2017; Williams et al., 2015). The typically wet, temperate northern California coast experienced particularly severe dry conditions during the 2014 drought event (Flint et al., 2018; Luo et al., 2017). This region, known for producing some of the tallest trees in the world, presents a unique ecosystem to study water resource dynamics in forested watersheds. In Australia, Saft et al. (2015) found that multiyear droughts could lead to changes in watershed function, with 43% of dry periods resulting in a significant downward shift in the relationship between precipitation and runoff. Endogenous mechanisms, such as mean watershed slope and percent woody cover, were found to be the main drivers of watershed function changes, whereas exogenous mechanisms, such as high temperatures and increased potential evapotranspiration, did not correlate with a significant change in watershed function (Saft et al., 2015). A follow-up study found that the historical aridity index, interannual groundwater variability, and soil depth all correlated well with changes the precipitation-runoff relationship (Saft et al., 2016).

Determining which characteristics of watersheds make them vulnerable to climatic disturbance and long-term change has become an area of active research, as long-term datasets and remote sensing have become more accessible (Aulenbach and Peters, 2018; Creed et al., 2014; Nippgen et al., 2016). Utilizing these tools has become vital to studying the existing variation in landscape characteristics within watersheds and their response to changes in precipitation to better inform future management.

One such source for long-term data is the Caspar Creek Experimental Watersheds (CCEW), an active research site since 1962, with well over 300 publications, reports, theses, and dissertations using data from the research site (Cafferata and Reid, 2013; Dymond et al., 2021a; Richardson et al., 2021). Numerous studies have been conducted investigating the relationship between forest harvest and streamflow at CCEW, however these studies often focus on peak flow (Keppeler et al., 2003; Reid and Lewis, 2009) or low flow (Coble et al., 2020), with some studies also examining annual water yield (Keppeler et al., 2024; Keppeler, 1998). CCEW began as a paired watershed study design, which later was shifted to include a sub-watershed design, comparing the streamflow response of smaller control and treatment catchments. Although this design is excellent at determining the effects of experimental treatments, this method can only tell us how a watershed behaves relative to another. It does not investigate the internal workings of a catchment, which may be mediated by the local topography, soil, and ecology. This study seeks to examine the rainfall-runoff relationship of headwater catchments in the CCEW, determining the influence of temporal variability, spatial variability, and disturbance on precipitation and streamflow dynamics.

2. BACKGROUND

2.1 Quantifying the Rainfall-Runoff Relationship

The field of watershed hydrology has developed several methods of investigating the rainfall-runoff relationship. The simplest approach is calculating the runoff ratio (RR), which is the ratio of streamflow normalized by watershed area (Q) divided by precipitation (P):

$$RR = \frac{Q}{P} \qquad \text{(Equation 1)}$$

RRs close to one indicate that the majority of the precipitation is reaching the stream, whereas RRs near zero imply that much of precipitation is lost to evapotranspiration (ET) or entering storage (S). RRs are largely determined by climate, as temperate regions like the Pacific Northwest have higher RRs with lower variability while more arid regions such as the Interior West had lower RRs with high variability (Chang et al., 2014).

This partitioning of P is described in the water balance equation, in which inputs must equal outputs in keeping with the law of the conservation of mass. In a mountainous watershed the equation is:

$$P = Q + ET + \Delta S \qquad \text{(Equation 2)}$$

Where P as the input, must equal the sum of Q and ET, assuming the change in storage (ΔS), held in soil or groundwater, is zero. ET and S are both recognized to be notoriously difficult to measure *in situ*, and thus the assumption that ΔS is zero allows for the estimation of ET. However, this assumption only holds at annual timescales or longer, as any stream flowing on a sunny day will demonstrate. Beyond the anecdotal, the foundational study of Hewlett and Hibbert (1963) demonstrated that an enclosed, sloping trough filled with 11 m^3 of saturated soil could produce outflow for over 140 days, thus proving the importance of soil water storage in sustaining baseflow.

Given the challenges of measuring S and ET, a promising alternative is examining precipitation history alongside streamflow to inform present hydrological response. By this logic, past P is incorporated into S and released as present Q to determine if a watershed has sufficient capacity in S to sustain Q. This storage capacity, often termed watershed memory, is a watershed characteristic which may determine resilience to precipitation variability over different time periods.

A form of this approach was applied in Nippgen et al. (2016), where lag-correlations between precipitation and runoff ratios found a significant relationship at monthly, seasonal (six month), and annual timescales. Notably, the previous year's precipitation was found to have an equally strong correlation with present runoff ratios as the present year's precipitation. At the seasonal time scale, the previous season's precipitation was found to have a stronger relationship with present runoff ratios on average. Though these results demonstrate the strong influence of past precipitation, correlating with runoff ratios, rather than streamflow itself, muddies the interpretation of these findings. Aulenbach and Peters (2018) have also utilized time series analysis of precipitation and runoff records to model monthly watershed storage and evapotranspiration. That study incorporated an event-scale baseflow recession analysis with a monthly water budget to determine the importance of shallow and deep-water storage in sustaining baseflow through drought conditions. These methods have been extended to examine regional trends in the rainfall-runoff relationship, which can inform models of ungauged watersheds (Chang et al., 2014; Moges et al., 2022).

2.2 Watershed Control on Rainfall-Runoff Relationship

Determining the source of runoff variability between catchments has been a perennial pursuit in the field of hydrology (Chang et al., 2014; Jones and Swanson, 2001; Merz and Blöschl, 2009; Nippgen et al., 2016). One of the most basic questions asked in watershed hydrology is: how does rainfall become streamflow? The partitioning of precipitation into streamflow, or the rainfall-runoff relationship, is complicated by a watershed's capacity to evapotranspire and store precipitation before it reaches the stream (Brown et al., 2005; Stednick, 1996). Watershed characteristics such as topography, soils, geology, and vegetation can mediate watershed function (as quantified by the rainfall-runoff relationship), leading to differences in water yield at the annual and sub-annual scale (Jones and Swanson, 2001; Saft et al., 2015; Segura et al., 2019). Large-scale disturbances such as timber harvest, wildfire, invasive species, insect infestation, and road building can also impact watershed function through landcover loss, vegetation regrowth, and changes in watershed connectivity (Rice et al., 2004; Wemple and Jones, 2003; Ziemer, 1981).

2.2.1 Topographic Effects

Topography fundamentally controls multiple avenues of a watershed's rainfall-partitioning. A watershed's elevation may determine how much precipitation a watershed receives, with higher elevation watersheds generally receiving more precipitation due to orographic uplift (Nippgen et al., 2016; Saksa et al., 2017). Additionally, evapotranspiration rates have a negative relationship with elevation, largely due to a decreasing temperature and vegetative index (Saksa et al., 2017). Minimum elevation was found to be a significant predictor of runoff ratio coefficient of variation in an analysis of watersheds across the contiguous United States (Chang et al., 2014). Elevation has been found to be a major factor in seasonal lag correlations between precipitation and runoff ratios, with lower elevation watershed's runoff ratios more strongly correlated to the previous six month season's precipitation and higher elevations more strongly correlated to the present (Nippgen et al., 2016).

Aspect is a primary determinant of how much solar radiation a hillslope will receive, and subsequently the evaporation rate (Yetemen et al., 2015). In the Northern Hemisphere, south-facing slopes which receive more solar radiation, have higher evaporation rates, as well as increased temperatures, with the reverse being true in the Southern Hemisphere. These environmental factors can both increase growth rates and vegetative stress, and lead to distinct biological communities (Desta et al., 2004). However, in humid regions, results show little to no aspect effect on runoff, indicating that this effect may only control water-limited systems (Nippgen et al., 2016).

Slope has been found to control a watershed's vulnerability to drought, with flatter watershed's having a significant transformation of their precipitation-runoff relationship (Saft et al., 2016). Slope was found to be a significant predictor in determining watershed runoff ratios across the United States (Chang et al., 2014). In a study conducted in Germany, at the hillslope scale, slope and aspect were shown to have higher explanatory power of water table variability than differences in vegetation (Bachmair and Weiler, 2012).

Topographic wetness index (TWI) is a commonly used metric which incorporates the local upslope contributing area and slope to topographic effects on hillslope hydrology (Beven and Kirkby, 1979), and is commonly used as a proxy for soil moisture. As an indicator of soil moisture, a watershed with a greater TWI may be expected to have greater runoff ratios as due to the transport of water through soil pores or conversely, lower runoff ratios due to the utility of soil water by vegetation (Loritz et al., 2019).

2.2.2 Vegetation and Harvest Impacts

Forests interact with watershed functioning through numerous pathways, some already briefly discussed (Creed et al., 2019). Vegetation intercepts precipitation, acting as temporary storage that can increase evaporation, prevent overland flow, and attenuate peak flows in streams (Keppeler et al., 2003; Reid and Lewis, 2009; Ziemer, 1981). Soil water is taken up by roots and transpired into the atmosphere, reducing the amount of water reaching the stream (Abdelnour et al., 2011; Hammerschmidt, 2020). In fog belts, such as along California's northern coast, foliage allows fog to condense, where it can be directly taken up by some species or dripped to the forest floor (Petreshen, 2021; Reid and Lewis, 2009). Such occult precipitation is challenging to measure and is assumed to be a minute component of the water budget, despite being ecologically significant (Baguskas et al., 2016; Chung et al., 2017).

Given the role of vegetation in watershed hydrology, vegetation disturbance, such as timber harvest, is known to impact these processes and has been a predominant focus of paired watershed studies (e.g., Brown et al., 2005; Jones et al., 2012; Jones and Swanson, 2001; Ziemer, 1998). Loss of forest coverage can increase peak flows in the short term as precipitation is no longer intercepted (Abdelnour et al., 2011; Keppeler and Lewis, 1998), although annual water yield can be unchanged if forest cover reduction is less than 20% (Stednick, 1996). As the forest regrows, young trees can consume more water than their older counterparts, resulting in decreased streamflow (Goeking and Tarboton, 2020; Perry and Jones, 2016). Perry and Jones (2016) found this effect particularly pronounced in the summer streamflow of old growth Douglas-fir stands converted to plantations, as younger trees had greater transpiration due to higher sapflow area, higher sapflow per unit of sapflow area, and high upper canopy leaf area concentration. A review of 78 hydrologic studies in Western coniferous forests revealed that post disturbance evapotranspiration may increase due to rapid vegetation regrowth as well as increase subcanopy radiation (Goeking and Tarboton, 2020). In addition, the review found water yield could vary substantially in response to vegetation disturbances, with increases, decreases, and no effect observed within and across studies. Shifts in species composition, due to ecological succession and replanting decisions, alongside changes in stand density, can also determine forest water use (Kerhoulas et al., 2020). Overall, the composition, density, and age of a forest stand can all be major factors that influence a watershed's water balance.

2.2.3 Soil and Geologic Effects

The soils and underlying bedrock geology largely determine the storage capacity of a watershed. Lithology is the primary determinant of groundwater storage, with more permeable and porous formations storing greater amounts of water (Hahm et al., 2019). However, jointing can provide pathways to transmit water and increase storage capacity in less permeable rocks, both in deep water storage, as well in shallow and exposed bedrock (McCormick et al., 2021). Geomorphic features, such as mass movement can store and release water on interannual timescales and provide baseflow during dry years (Segura et al., 2019). Within the stream channel, channel aggradation may increase hyporheic flow resulting in a loss of surface flow (Asarian and Walker, 2016).

Soil water storage is a major contributor to streamflow, allowing even watersheds with impermeable bedrock to maintain baseflow through dry periods (Hewlett and Hibbert, 1963). Storage and transmission of water in soil are largely dependent on the soil texture, porosity, bulk density, and depth (McGuire et al., 2024). For example, soils with greater clay content tend to have greater porosity and allow for more infiltration and storage of water compared to sandy soils. In seminal paper, Hewlett and Hibbert (1963) saturated a 13 meter inclined trough of soil and observed 145 days of outflow before the experiment was terminated. Notably, the soil mass reached an unsaturated state within 5 days, however nearly a quarter of the total outflow was sourced from unsaturated flow. Extrapolating to the watershed scale, this experiment demonstrated that baseflow could be sustained by soil water, even in unsaturated conditions. Within the Northern California region, an investigation comparing the watershed processes between the Coastal Belt and the Central Belt of the Franciscan Complex determined that the more deeply weathered Coastal Belt was able to sustain baseflow through the summer, while the Central Belt with a thinner critical zone, exhibited greater peak storm flows and little summer baseflow (Hahm et al., 2019). These differences in lithology are determinant to the vegetation ecology overlying the geologic units, despite similar precipitation patterns.

Soil and slope position may also interact — at the Caspar Creek Experimental Watersheds in coastal northern California, ridgetops with gentler slopes and deeper soils were found to remain wetter in the wet season than shoulder sites with steeper slopes and shallower soils (Dymond et al., 2021b). Whether this interaction affects annual water yield has yet to be determined. Soil piping, a macropore formed by various chemical, physical, and biological processes, can create highly efficient subsurface flow paths that may route water away from entering long-term storage (Keppeler and Brown, 1998; Ziemer and Albright, 1987).

2.3 Drought

2.3.1 Disturbance and Ecological Effects

Drought is a disturbance event that is at once commonly understood and loosely defined. In general, drought is caused by a temporary and significant reduction in precipitation that a region receives (Mishra and Singh, 2010). Droughts can occur over a season, a year, or several years, but must be an anomaly from the normal regional climate. This is in contrast with the characteristic of aridity, in which the normal climate is one with low precipitation (Wilhite and Glantz, 1985). Although droughts are primarily driven by a loss in precipitation, they may be exacerbated by increased temperatures, high winds, and low relative humidity. Human factors such as increasing populations, land use change, and mismatches in precipitation timing and water need, are leading to the increasing frequency of droughts globally (Chiang et al., 2021). As with many natural hazards, climate change plays a part in the increased frequency of droughts, however modelling future shifts in precipitation has proven difficult (Keyantash and Dracup, 2002; Wang et al., 2017).

2.3.2 Drought in California

In typical years, California has a distinct wet season from October to May and corresponding summer dry season. Storms form in the Eastern Pacific and travel with the prevailing westerly winds to bring precipitation across the state. The region is prone to periods of drought, however climate change may be driving changes in precipitation patterns that could lead to more frequent and extreme drought (Swain et al., 2014; Swain, 2021; Wang et al., 2017). In Northwestern California, an analysis spanning 1953-2012 found that although less than 10% of study sites had significant long-term decreases in annual precipitation, changes in monthly precipitation were common (Asarian and Walker, 2016). For example, 70% of sites saw a significant decrease in September precipitation. The Eel River Basin, adjacent to our study area, additionally saw declines in January and August, and increased precipitation from May through July. These sub annual changes in precipitation patterns could result in ecological impacts such as mismatched timing of fish migration, plant germination, and bloom periods (Bartolini et al., 2019; Kelson and Carlson, 2019; White et al., 2009). The CCEW has experienced three meteorological and hydrological droughts since its establishment in 1962 (Keppeler et al., 2024).

From 2012 to 2015, California experienced widespread drought that peaked in 2014. The drought was caused by a ridge of high pressure developing along the west coast that curbed precipitation (Seager et al., 2015; Swain et al., 2014; Williams et al., 2015). Unsurprisingly, precipitation deficits were the key driver in drought severity, however the state also experienced anomalously high temperatures over the same period (Luo et al., 2017). Though there is general agreement that meteorological drought was the main mechanism that drove the hydrological and agricultural drought, studies have disagreed as to the contribution of anomalously high temperatures to the drought severity, with estimates ranging from 1 to 27% (Luo et al., 2017; Seager et al., 2017; Williams et al., 2015). This discrepancy has largely been attributed to differences in the drought indices used, as well as different time periods over which "normal" temperatures were established.

Despite these differences in driving factors, the overall severity of the drought should not be understated. Robeson (2015) found the drought to be the most severe in NOAA's records going back to 1895, and tree ring records indicated the return period of the event was greater than 10,000 years. The drought resulted in the death of 102 million forest trees, due to low soil moisture levels and reductions in flow coupled with higher stream temperatures caused a significant loss to the 2014 and 2015 cohorts of winter run

Chinook salmon (Lund et al., 2018). The total economic cost of the drought is estimated to be $2.7 billion in losses with 21,00 total job losses.

Given the significant ecological and economic costs of drought, it is imperative that we investigate the effects of drought at the watershed scale. Determining what biophysical factors may mitigate the consequences of this disturbance could help more efficiently direct resources for response and management as drought events become more common into the future.

3. STUDY OVERVIEW

3.1 Study Site

The Caspar Creek Experimental Watersheds (CCEW; 39°21’N, 123°44’W) are located within the Jackson Demonstration State Forest (JDSF) in Mendocino County, California (Figure 1). The experimental watersheds were established in 1962 by the US Forest Service Pacific Southwest Research Station (PSW) and California Department of Forestry and Fire Protection (CAL FIRE) to investigate impacts of timber harvesting on watershed processes. The study area is split between the North Fork (473 ha) and South Fork (424 ha) tributaries of Caspar Creek.

Caspar Creek has a coastal Mediterranean climate with over 90% of the precipitation falling as rain from October to April, and rare snowfall (Keppeler et al., 2024). Summers are relatively dry with moisture predominantly provided by coastal fog. Drought generally affected the region from 2012 to 2014 (Keppeler et al., 2024; Luo et al., 2017). Elevations within the watershed range from 37 to 330 m and the topography is relatively steep with average slopes ranging from 15° to 35°. The watersheds are underlain by the Cretaceous marine deposits of the Franciscan Formation (NRCS, 2002). These consist of greywacke sandstone and coarse-grained shale. The soil averages 1-2 meters thick and is generally composed of well-drained sandy clay loams (Dymond et al., 2021). Soil pipes have been observed in parts of the watershed that aid in water transport and streamflow generation (Keppeler and Brown, 1998).

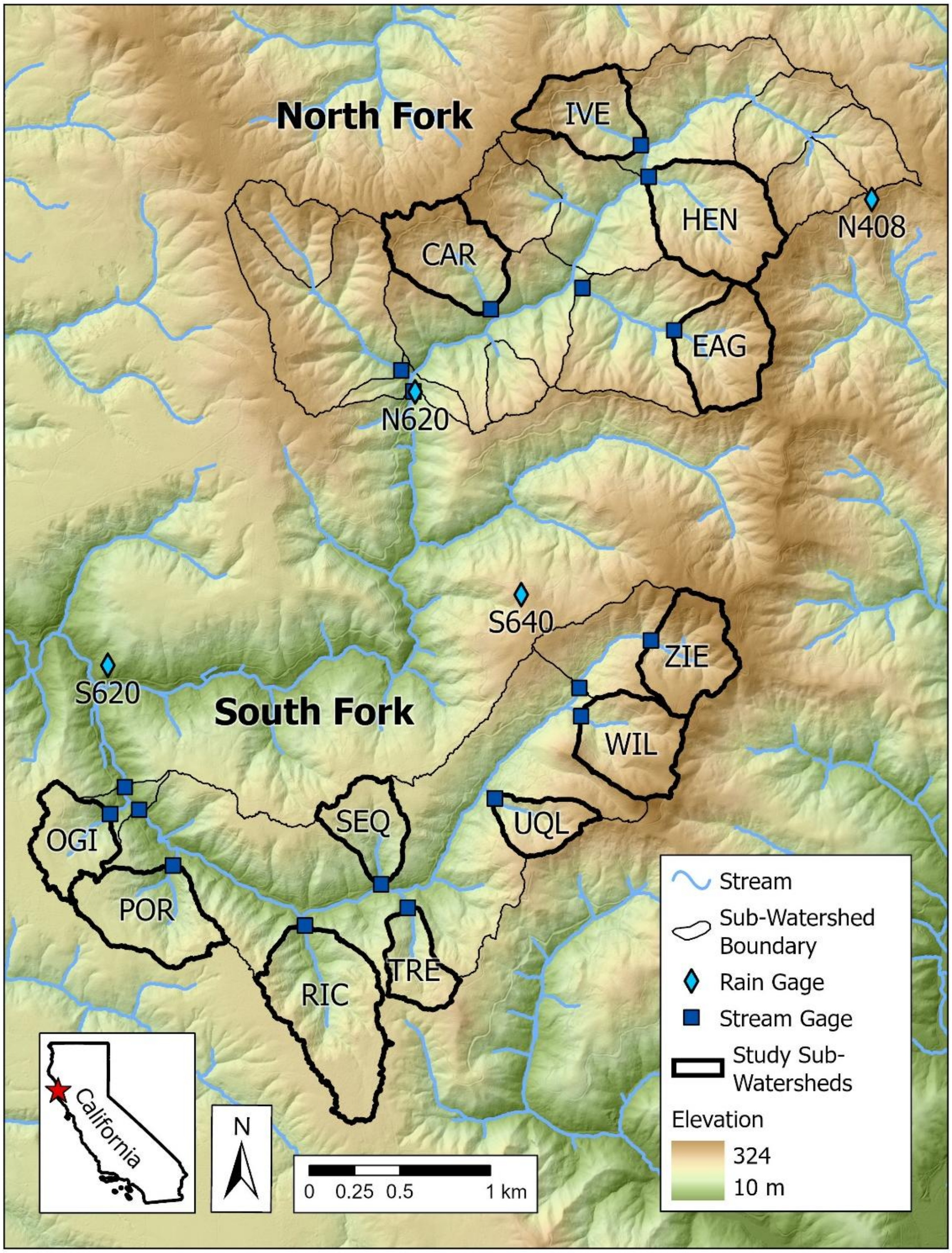

Figure 1. The eight sub-watersheds within the Caspar Creek Experimental Watersheds chosen for the study have variation in harvest history as well as topographic characteristics.

The forest at Caspar Creek is primarily composed of 2nd to 4th-growth coast redwood (*Sequoia sempervirens* (D. Don) Endl.), Douglas-fir (*Pseudotsuga menziesii* (Mirb.) Franco), grand fir (*Abies grandis* (Doug. Ex D. Don Lindl.), and western hemlock (*Tsuga heterophylla* (Raf.) Sarg.). The Caspar Creek watershed underwent extensive logging from the 1860s until 1904. Once the secondary forest matured, the first experiment at Caspar Creek involved a selection harvest of 63% of the South Fork watershed between 1971 and 1973 (Rice et al., 1979). From 1985 to 1991, a second experiment clearcut select sub-watersheds of the North Fork with varying riparian corridor widths (Ziemer, 1998b). The third experiment, which harvested six of the sub-watersheds of the South Fork, began in the spring of 2017 (Dymond et al., 2021a).

3.2 Study Questions

The goal of this study is to determine how the rainfall-runoff relationship of sub-watersheds in Caspar Creek is affected by past precipitation, watershed properties, and drought. The specific research questions and hypotheses are detailed below.

Question 1: How does past precipitation affect present runoff at annual, seasonal, and monthly timescales?

Hypothesis 1_0*:* There is no effect from past precipitation on present runoff.

Hypothesis 1_A*:* Past precipitation will have a positive correlation with present runoff with decreasing significance as the number of lags increase. The strength of the correlation will be stronger over smaller timescales.

Explanation: Sufficient storage in the system allows past precipitation to determine present runoff.

Question 2: What sub-watershed properties (topography, soil, and stand structure) drive differences in annual runoff ratios among sub-watersheds?

Hypothesis 2_0: No variable significantly explains variation in water yield among sub-watersheds.

Explanation: An extended wet season and fog in the dry season will offset any effects of solar radiation on aspect. Soil characteristics and stand structure metrics do not have enough variability to impact streamflow.

Hypothesis 2_A: Topography (elevation, aspect, and slope) is the main driver of variability in runoff ratio among sub-watersheds.

Explanation: Topographic variation can alter the amount of precipitation a sub-watershed receives, the degree of solar radiation and evaporation that occurs, and the connectivity with the stream.

Hypothesis 2_B: Variations in soil texture and depth are the main drivers of differences in water yield among sub-watersheds.

Explanation: Soil texture and depth can determine the infiltration rate and storage capacity of a watershed. These variables may also be connected to evapotranspiration rates.

Hypothesis 2_C: Variations in stand density and past harvest disturbance are the main drivers of differences in water yield among sub-watersheds.

Explanation: Stand density can determine evapotranspiration rates and precipitation interception. Past harvest disturbance may influence stand density, stand age, and species composition, which may all affect evapotranspiration rates.

Question 3: How does anomalously low annual precipitation (dry years) affect runoff ratios of sub-watersheds?

Hypothesis 3_0: Dry years will not have significantly different runoff ratios from other years.

Explanation: Declines in annual precipitation will cause proportional declines in streamflow, resulting in no change in sub-watershed runoff ratios.

Hypothesis 3_A: Dry years will have significantly lower runoff ratios compared to other years.

Explanation: In dry years, evapotranspiration rates will remain constant due to unchanged watershed area and stand density, or increase due to decreased humidity, resulting in a greater proportion of precipitation being lost to evapotranspiration. Lower annual precipitation will produce less streamflow and subsequently lower sub-watershed runoff ratios.

Hypothesis 3_B: Dry years will have significantly higher runoff ratios compared to other years.

Explanation: Baseflow from watershed storage will buffer streamflow responses, despite anomalously low annual precipitation, resulting in proportionally greater streamflow compared to precipitation, and thus increased runoff ratios.

Question 4: How does anomalously low annual precipitation interact with variation in sub-watershed characteristics to impact annual runoff ratios of sub-watersheds?

Hypothesis 4_0: There is no interaction between annual precipitation variability and sub-watershed variability that impacts annual runoff ratios.

Hypothesis 4_A: There will be a significant interaction between sub-watershed characteristics and annual precipitation.

Explanation: Differences in sub-watershed characteristics will determine the degree to which runoff ratios shift during anomalously low precipitation years.

4. METHODS

4.1 Hydroclimate Datasets

The North and South Fork watersheds are divided into 16 and 11 sub-watersheds, respectively (Figure 1). Sub-watersheds for this study were chosen for having complete streamflow records during the study period and for being headwater catchments. Headwater catchments were selected to avoid cumulative effects of nested catchments. Of the 27 sub-watersheds in CCEW, 12 were used in the study: four in the North Fork (CAR, EAG, HEN, and IVE) and eight in the South Fork (OGI, POR, RIC, SEQ, TRE, UQL, WIL, and ZIE). All annual hydroclimate data were calculated for the hydrologic year (HY), which was defined as starting October 1 of the preceding calendar year, with the study starting in HY-2001 and ending HY-2017. Seasonal hydroclimate data were categorized as “wet” from December to March and “dry” from June to September, with shoulder season months excluded. These definitions were based on previous work in the CCEW which examined whether or not total monthly precipitation exceeded Thornthwaite potential evapotranspiration (PET; Dymond et al., 2021b; Thornthwaite, 1948).

Precipitation data were collected at four long term rainfall stations within the Caspar Creek Experimental Watershed — North Fork 408 (nfc408), North Fork 620 (nfc620), South Fork 620 (sfc620), and South Fork 640 (sfc640; Richardson et al., 2022). Rainfall was measured using tipping-bucket rain gages, which record the time of each 0.025 cm tip. Precipitation for each rainfall station was calculated by summing the total precipitation within each time step (i.e., hydrologic year, season, or month) in the study period. Precipitation for each sub-watershed was calculated using the nearest rain gage to the geographic center of the sub-watershed. Other methods for estimating catchment rainfall were found to be inappropriate for this analysis. Specifically, Thiessen polygons did not result in a significantly different record for any sub-watershed, the hypsometric method found no significant relationship with elevation, and spatial interpolation approaches could not be used due to the need to extrapolate outside the rain gage network in order to cover all of the sub-watersheds. The more sophisticated Parameter-elevation Relationships on Independent Slopes Model (PRISM) was considered as an alternative to locally measured rainfall, however the model over estimated annual precipitation during drought years at the study site (PRISM Climate Group, 2017).

Stream depth at each sub-watershed outlet has been measured using Montana flumes at 10-minute intervals, beginning in 1985 for the North Fork sub-watersheds and 2000 for the South Fork sub-watersheds (Dymond et al., 2021a). Flow depth was then converted to volumetric discharge using stage-discharge rating equations. Water yield was calculated at annual, seasonal and monthly timescales by summing the daily average discharge across the timestep and dividing by the sub-watershed area. All calculations and subsequent analyzes were performed in R version 4.1.2. (R Core Team, 2021).

The annual time series for each precipitation and streamflow dataset were tested for trends over time using a linear regression analysis to determine suitability for time series analysis. All rain and streamflow gages except EAG did not have significant trends over the study period ($p < 0.05$). It had an adjusted R^2 of 0.21, indicating a sufficiently weak relationship. The EAG sub-watershed trend appeared to be driven by higher-than-average values from 2001-2004, as the trendline is insignificant if these years are excluded.

Annual, seasonal, and monthly runoff ratios for each sub-watershed were calculated by dividing the runoff by the precipitation (Equation 1). Due to precipitation and streamflow frequently reaching zero during the summer months, monthly runoff ratios often were undefined (equaling infinity or not a number). As such, examining monthly runoff ratios was determined to be inappropriate for analysis. However, a modified average monthly runoff ratio ($\overline{RRm}$) was constructed by finding the ratio of each sub-watershed's average monthly streamflow and precipitation (Equation 3). This construction aided in demonstrating differences between sub-watersheds, particularly in the dry season, however it was not used in further analysis due to reduced sample size.

$$\overline{RRm} = \frac{Q_{avg}}{P_{avg}} \qquad \text{(Equation 3)}$$

For annual runoff ratios, a Sample Autocorrelation Function test was applied to the data using R package astsa (Stoffer, 2021), and determined that only the EAG sub-watershed had significant autocorrelation at a lag of 1 year ($p < 0.05$). This autocorrelation had an adjusted R^2 of 0.23, indicating again a relatively weak relationship. Thus, all sub-watersheds annual runoff ratios were tested as independent samples. Runoff ratios for each sub-watershed were tested for normality visually using histograms and Q-Q plots, as well quantitatively using a Shapiro-Wilkes test. All except the sub-watershed POR exhibited a normal distribution ($p < 0.05$), however the assumption of normality needed for parametric statistical analysis is robust and the distribution of POR appeared visually near-normal. As such, parametric tests were deemed appropriate for subsequent analysis.

4.2 Sub-Watershed Properties

Topographic characteristics of each sub-watershed were derived from a LiDAR-based digital elevation model (DEM) using ESRI ArcGIS Pro software (Table 1; Richardson et al., 2020). Elevation variables were sampled at the 1 m resolution to avoid underestimations. The DEM was resampled to a 10 m resolution for the remaining topographic variables to smooth effects of microtopography. The mean, minimum, and maximum of elevation, slope, and topographic wetness index (TWI; Equation 4) were calculated for each sub-watershed, as well as the mean aspect (Beven and Kirkby, 1979). TWI was calculated as:

$$TWI = ln\frac{\mathrm{a}}{\tan \mathrm{b}} \qquad \text{(Equation 4)}$$

where *a* is the upstream flow accumulation area in square meters and *b* is the local slope in radians.

Table 1. Topographic statistics of the sub-watersheds in the study. Standard deviation is abbreviated as SD.

Sub-Watershed	Area (ha)	Elevation (m)			Slope (°)			Aspect (°)	TWI		
		Mean	Range	SD	Mean	Range	SD	Mean	Mean	Range	SD
CAR	29.0	217	83-299	51	22	0-45	9	145	4.9	2.5.-12.5	1.5
EAG	26.7	235	126-306	44	25	1-42	7	280	4.6	2.4-12.3	1.6
HEN	38.0	214	104-306	49	22	0-38	7	306	4.8	2.5-14.2	1.6
IVE	23.2	215	110-303	45	25	1-42	9	124	4.7	2.5-12.1	1.5
OGI	19.2	149	55-175	25	13	0-37	9	51	5.7	2.6-12.5	1.6
POR	30.5	140	41-188	34	17	0-45	11	23	5.2	2.4-12.8	1.7
RIC	46.7	155	48-203	43	20	0-43	13	2	5.2	2.4-14.6	1.9
SEQ	17.2	149	57-193	35	18	0-43	10	167	5.2	2.5-11.5	1.5
TRE	14.2	160	70-230	35	23	0-42	11	353	4.8	2.4-11.3	1.6
UQL	12.9	205	99-279	39	24	2-43	8	299	4.6	2.5-11.1	1.5
WIL	26.3	237	133-324	44	25	1-42	8	304	4.6	2.5-12.6	1.5
ZIE	24.3	266	184-324	32	21	0-41	9	273	4.8	2.5-12.9	1.5

Two forest stand metrics were used to describe the forest vegetation across watersheds: basal area (BA) and stand density index (SDI). BA is the cross-sectional area of a stem and is converted from diameter at 1.37 m height (DBH) based on the area of a circle. The formula for mean BA (m^2 per ha) across a watershed is:

$$BA = \sum 0.00007854 * ND^2 \qquad \text{(Equation 5)}$$

Where N is the average stems per hectare and D is the DBH class (cm). SDI, on the other hand, is a unitless expression of the density of trees relative to their diameter (Reineke, 1933):

$$SDI = \sum N \frac{D}{25.4}^{-1.605} \qquad \text{(Equation 6)}$$

Forest inventory surveys were conducted across the watersheds in 2017 by CAL FIRE. Survey plots were placed on a square grid with one plot per four ha (10 ac) in the North Fork and a variable one to five plots in the South Fork (CAL FIRE, 2016). Due to these differences in survey intensity, we were able to calculate BA and SDI for each sub-watershed in the South Fork, however in the North Fork, BA and SDI were calculated for each sub-watershed based on their Experiment 2 treatment (uncut or cut). DBH for all stems greater than 10 cm (4 in.) was measured in each plot. Stems were binned into DBH classes every 5 cm (2 in.), and plots were aggregated to determine average number of stems per acre by each DBH class. BA and SDI were derived for each DBH class and summed to find the mean BA (Equation 5) and SDI (Equation 6) for each sub-watershed.

Metrics for harvest disturbance included the last harvest year, harvest type, and percent area logged, which were based on the treatments used in Experiments 1 and 2.

Table 2. Forest stand data for each sub-watershed. Basal area and stand density index values are from surveys conducted in 2017. Percent logged is the percent of basal area removed in the harvest.

Sub-Watershed	Harvest Disturbance	Harvest Type	Last Harvest Year	Percent Logged	BA (m^2 per ha)	SDI
CAR	Experiment 2	Clearcut	1991	96	48.6	336
EAG	Experiment 2	Clearcut	1991	100	48.6	336
HEN	Control	none	1900	0	99.4	539
IVE	Control	none	1900	0	99.4	539
OGI	Experiment 1	Selection	1971	50	75.1	485
POR	Experiment 1	Selection	1971	54	78.7	489
RIC	Experiment 1	Selection	1972	67	87.2	508
SEQ	Experiment 1	Selection	1972	67	95.0	562
TRE	Experiment 1	Selection	1972	67	93.6	531
UQL	Experiment 1	Selection	1973	67	77.8	483
WIL	Experiment 1	Selection	1973	67	99.2	588
ZIE	Experiment 1	Selection	1973	67	85.8	532

Soils data were obtained from the Natural Resources Conservation Service (NRCS) Western Mendocino County database (NRCS, 2002). Soil map units were clipped to the extent of the study area and the percent area of each soil complex was determined for each sub-watershed using ArcGIS Pro 2.8.2 (Figure 2). Within each complex, the percent area, soil texture, and maximum soil depth of each soil series was determined from the available metadata. For series where soil texture was not included in the description, percent sand, silt, and clay were used to determine the USDA texture classification. Organic and bedrock horizons were omitted from the soil texture and depth calculations. The soil texture and maximum soil depth for each soil series complex was weighted based on the percent area in each sub-watershed (Table 3).

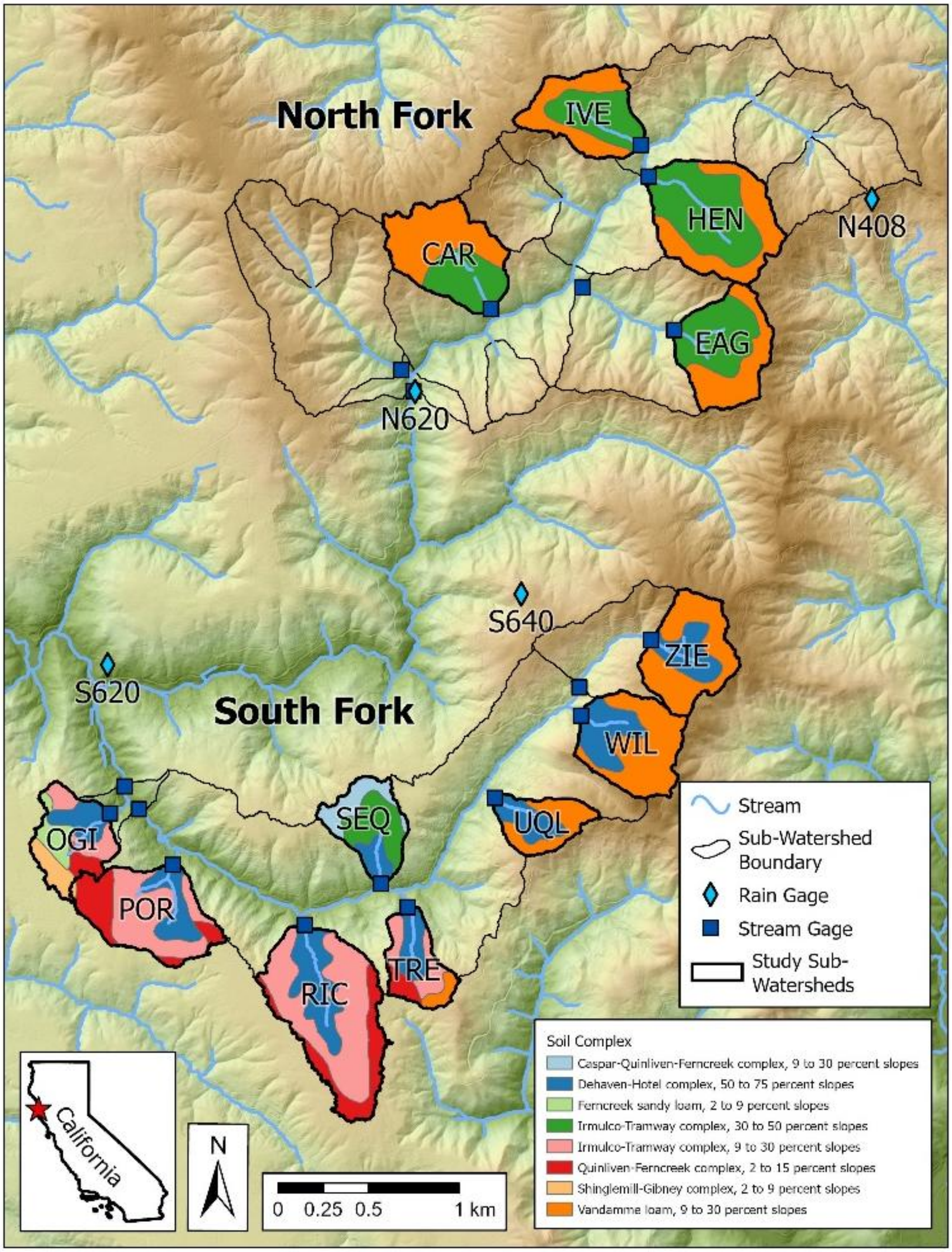

Figure 2. Soil complexes of the Caspar Creek sub-watersheds.

Table 3. Mean soil characteristics of each sub-watershed.

Sub-Watershed	Primary Soil Series	Mean Depth (cm)	Mean Sand (%)	Mean Silt (%)	Mean Clay (%)	USDA Texture
CAR	Vandamme	118.2	31.9	31.0	34.2	Clay Loam
EAG	Irmulco	122.8	32.7	32.1	32.7	Clay Loam
HEN	Irmulco	124.5	33.0	32.4	32.2	Clay Loam
IVE	Irmulco	121.5	32.5	31.8	33.1	Clay Loam
OGI	Dehaven	141.7	45.1	26.2	29.4	Sandy Clay Loam
POR	Irmulco	136.6	41.5	29.5	29.2	Clay Loam
RIC	Irmulco	133.7	40.7	30.3	29.0	Clay Loam
SEQ	Irmulco	139.0	43.4	28.8	27.6	Clay Loam
TRE	Irmulco	126.7	40.1	29.7	29.7	Clay Loam
UQL	Vandamme	109.9	36.2	29.0	32.8	Clay Loam
WIL	Vandamme	109.3	34.9	28.9	33.9	Clay Loam
ZIE	Vandamme	109.1	34.3	28.9	34.3	Clay Loam

4.3 Statistical Analyses

4.3.1 Past Precipitation Lag Analysis

A lag-correlation analysis was performed at multiple timescales to determine the impact of past precipitation on present runoff. The effect was examined at annual, seasonal, and monthly timescales. Seasons were defined as “wet” from December to March and “dry” from June to September. A second lag-correlation analysis was performed between past precipitation and present runoff ratios, however the monthly timescale was excluded. This was due to a large portion of monthly runoff ratios being undefined as there was no precipitation measured in these months. As such, the lag-correlation analysis would have been an inappropriate test.

A Pearson lag-correlation coefficient (r_p) was calculated between precipitation and runoff or runoff ratio, using the R stats package (R Core Team, 2021). Lags of precipitation were calculated such that a lag of zero was the current timestep’s precipitation and a lag of one indicated the present runoff or runoff ratio was being correlated to the previous timestep's precipitation. Correlations were calculated up to six lags at the annual scale (n = 17), twelve lags at the seasonal scale (n = 32), and 24 lags at the monthly scale (n = 204).

4.3.2 Watershed Property Effects on Runoff Ratios

An Analysis of Variance (ANOVA) was used to determine if any watershed properties were significant determinants of runoff ratios ($\alpha = 0.05$), using the "stats" package in R (R Core Team, 2021). ANOVA was used to compare across categorical and continuous variables. All watershed properties, except for harvest disturbance and mean aspect, were binned into "high", "mid", and "low" bins, using natural breaks in the distribution of the data (Table 4). Data was binned to make results both categorical and continuous comparable. Due to the correlation of the harvest disturbance variables within each experimental treatment, sub-watersheds were binned for general harvest disturbance as "control", "Experiment 1", or "Experiment 2." Mean aspect was binned as north-, west-, and south-facing, using natural breaks (Figure 3). An Akaike Information Criterion (AIC) test was used to determine which of the significant variables presented the best fit model (Akaike, 1974). A Tukey's Honest Significant Difference (HSD) test using the "agricolae" R package then determined of the best fit models, whether any bins had significantly different runoff ratios ($\alpha = 0.05$; de Mendiburu, 2021; Tukey, 1949). Watershed properties were ultimately determined to be significant (nonzero) predictors based on the results of the statistical tests, as well as the logic of their direction and order.

Explanatory variables with statistical significance, but without a mechanism to explain their direction or order of their groupings were determined to be false positives.

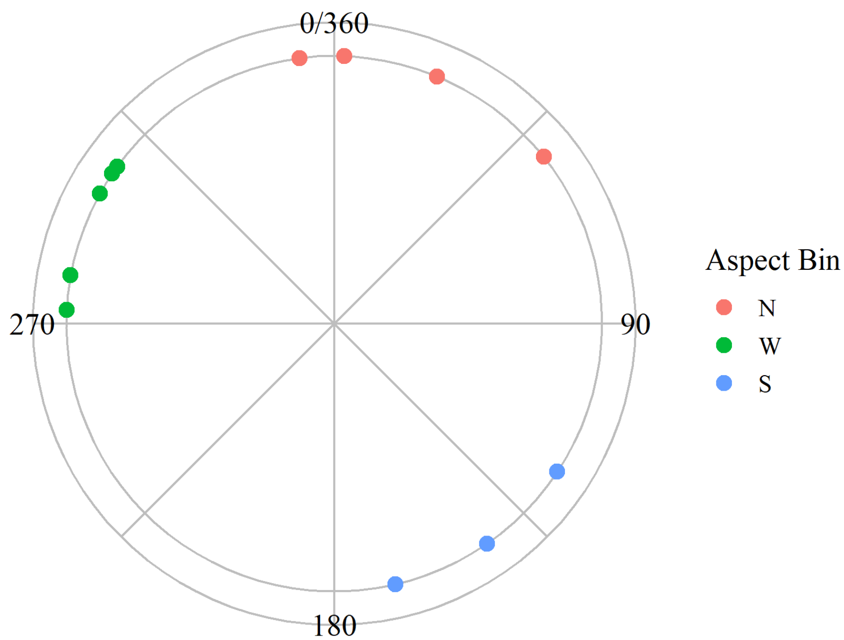

Figure 3. Mean aspect of each sub-watershed, showing values assigned to the North, South, and West groups. No sub-watersheds were grouped as East.

Table 4. Sub-watershed properties tested in ANOVA of runoff ratios, with ranges used for categorical binning.

Sub-watershed Property	Low	Mid	High
Watershed Area (ha)	12-20	20-28	28-48
Mean Elevation (m)	130-180	180-230	230-280
Elevation Range (m)	110-150	150-190	190-230
Mean Slope (°)	12-18	18-23	23-29
Mean TWI	4.5-4.74	4.74-5.15	5.15-5.7
Total SDI*	330-430	430-530	530-630
Total BA (m2/ha)	45.9-68.9	68.9-91.8	91.8-114.8
Mean Soil Depth (cm)*	109-118	118-130	130-142
Harvest Disturbance	Control	Experiment 1	Experiment 2
	N	W	S
Mean Aspect (°)*	350-55	270-305	123-180

* $p < 0.05$

4.3.3 Impact of Dry Years on the Runoff Ratios

To understand the impact of drought on hydrologic function, runoff ratios were compared between dry and normal years. Dry years were determined to be any year in which the mean of the four rain gages was greater than one standard deviation below the mean of the rain gages over the study period (Figure 4). The mean of the rain gages was used to smooth out variability across the gages. A Welch Two Sample t-test was performed to determine if there were significant differences in the mean runoff ratios of all sub-watersheds between dry and normal years (α = 0.05), using the stats package in R (R Core Team, 2021). A Standardized Precipitation Index (SPI) was not used as the precipitation records for all gages were shorter than the 50-year record recommended (Guttman, 1999; Keppeler et al., 2024).

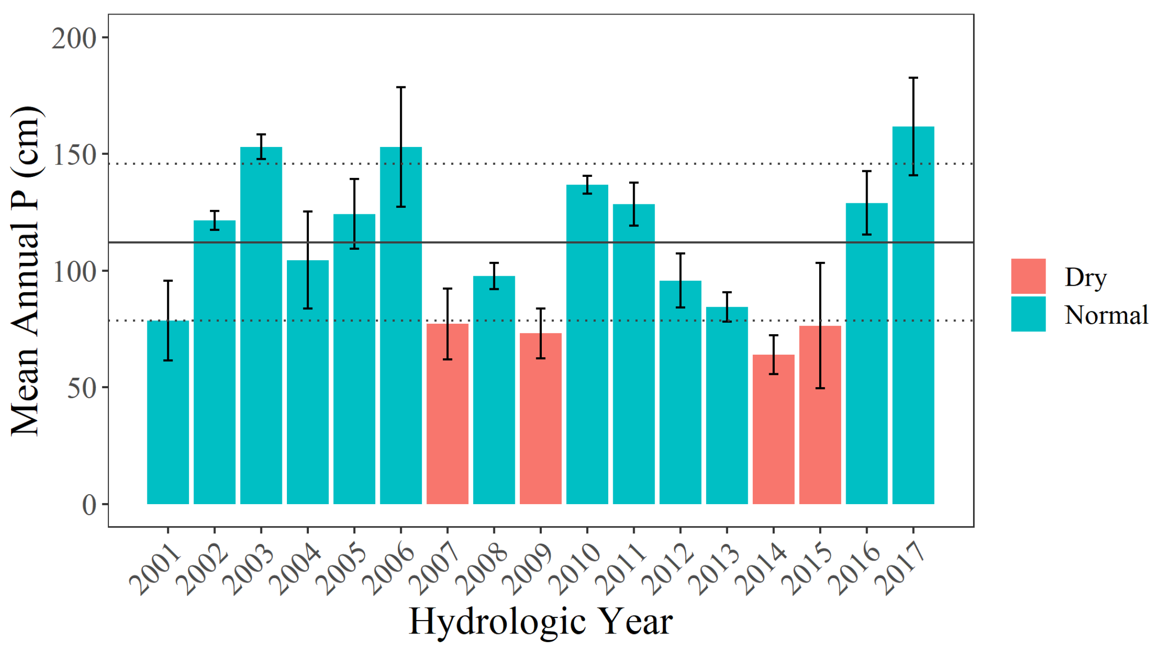

Figure 4. Mean annual precipitation across the four gauges used in the study for the study period. The solid line indicates the mean precipitation of all gages during the study period and the dashed lines show one standard deviation from the mean.

4.3.4 Combined Effects of Drought and Watershed Properties on Runoff Ratios

To determine which watershed properties provided resilience to drought, two-way ANOVAs were performed in which dry and normal precipitation years were combined with a watershed property to determine if there were significant differences in the mean runoff ratios ($\alpha = 0.05$). Only watershed properties (aspect, SDI, and soil depth) were found to be significantly correlated with annual runoff ratios were tested (Table 4). An AIC was used to compare the models to determine the best fit. A Tukey's HSD test then determined how to group the bins with significantly different runoff ratios ($\alpha = 0.05$) of the best fit models.

5. RESULTS

5.1 Hydroclimate Time Series

5.1.1 Precipitation

Monthly precipitation data showed a clear seasonal pattern as precipitation on average increased beginning in October, peaked in December, remained steady January through March, and declined towards zero by the summer months (Figure 5). On average, 75.6% of precipitation fell in the wet season from December to March, while 3.2% fell in the dry season from June through September. There was a greater spread in the average monthly precipitation measured at each gage during months with greater rainfall, with S640 consistently recording the highest monthly rainfall. The other three gages were variable across the wet season as to which measured the most or least rainfall. Notably, the months of October, November, and April received approximately the same average amount of rainfall, however there was greater variability among the gages during October and November as compared to April.

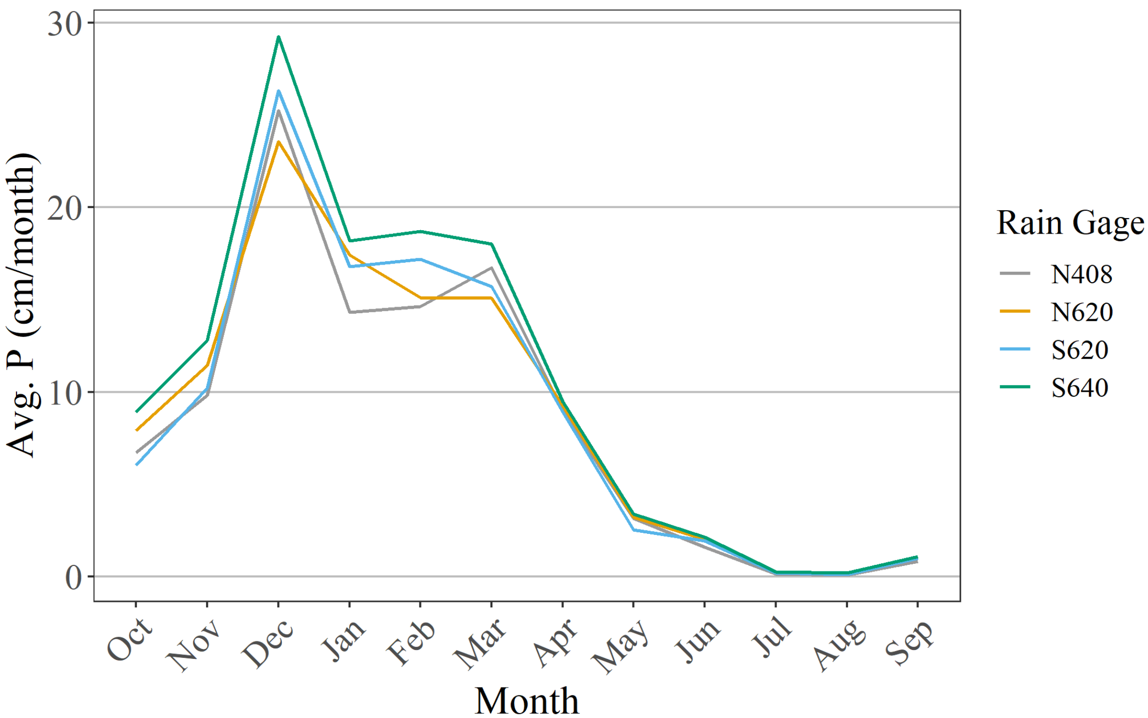

Figure 5. Average monthly precipitation of each rain gage over the hydrologic year, with precipitation peaking in December and approaching zero by July.

Monthly precipitation over the study period demonstrated that though on average precipitation peaked in December, there was considerable variability across years and between gages (Figure 6). Water years 2002, 2012, 2013, and 2014 showed relatively similar measurements between gages, while 2003, 2006, and 2017 showed greater differences between gages.

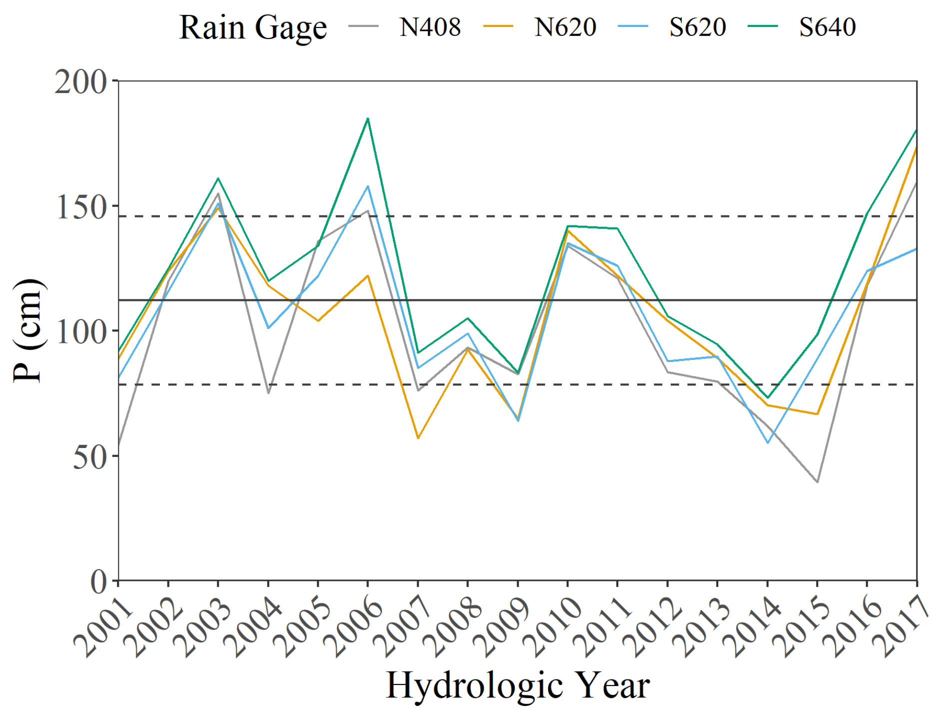

Figure 6. Annual precipitation by rain gage. The record mean and standard deviation across the gages are shown by the solid and dashed lines, respectively.

Annual precipitation over the seventeen-year study period averaged 109.4 cm (σ = 33.6 cm) across the gages, while average precipitation from 1963 to 2022 for the CCEW was 114.6 cm, indicating that the study period was relatively drier than the longer-term record (Figure 7; Keppeler et al., 2024). Gage S640 had the highest annual mean (122 cm), while N408 had the lowest annual mean (102 cm). Conversely, N408 had the greatest variation in annual precipitation (σ = 37 cm; Table 5), while S620 had the least (σ = 29 cm). The lowest annual rainfall was 39.4 cm, recorded at gage N408 in 2015, while the lowest average across the stations was 65.2 cm in 2014. The highest annual rainfall was 185.2 cm, recorded at gage S640 in 2006, however the highest average across stations was 162.1 cm in 2017.

Table 5. Study period annual mean and standard deviation of precipitation, runoff, and runoff ratios of each sub-watershed and corresponding rain gage.

Sub-Watershed	Rain Gage	Precipitation (cm)		Runoff (cm)		Runoff Ratio	
		Mean	SD	Mean	SD	Mean	SD
CAR	N620	106	32	56.7	33.8	0.500	0.205
EAG	N408	102	37	61.9	39.2	0.602	0.320
HEN	N408	102	37	54.5	38.0	0.506	0.249
IVE	N408	102	37	54.0	29.3	0.518	0.172
OGI	S620	107	29	68.6	32.5	0.624	0.171
POR	S620	107	29	62.6	29.5	0.563	0.134
RIC	S620	107	29	53.7	26.5	0.478	0.122
SEQ	S640	122	34	44.0	25.0	0.334	0.112
TRE	S640	122	34	72.6	32.3	0.569	0.109
UQL	S640	122	34	51.7	26.6	0.397	0.111
WIL	S640	122	34	52.6	27.4	0.405	0.109
ZIE	S640	122	34	60.0	30.4	0.462	0.123

The monthly precipitation shows the extreme variability in rainfall distribution over the study period (Figure 7). Most years show at least one month, typically December, with rainfall greater than 20 cm/month and more moderate, however variable amounts of rainfall from January through April (see also Figure 5). However, dry years show a delay in rainfall with less pronounced peaks in December (2007, 2009, and 2014) or greater variability across gages in that month (2015).

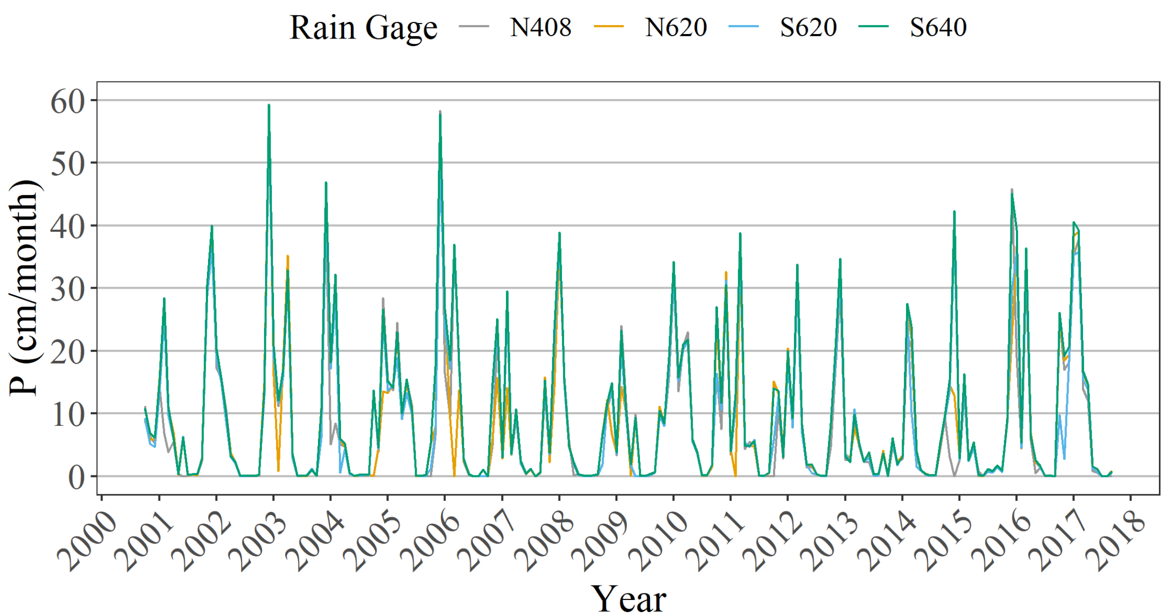

Figure 7. Monthly precipitation of each rain gage over the study period.

Precipitation means at the gages did not have a significant relationship with elevation (α = 0.05). Additionally, unlike at the monthly timescale, there was a lack of consistent order across the gages such that no gage received consistently more or less precipitation than any other gage year-to-year. An ANOVA demonstrated that there were significant differences between hydrologic years, but not between rain gages over the study period (α = 0.05).

5.1.2 Runoff

As with the average monthly precipitation data, the average monthly streamflow data showed a clear seasonal pattern of peak winter flows and summer low flows (Figure 8). Most sub-watersheds had the highest average flow in December, with the exception of

IVE and OGI, which both peaked in March. All watersheds had an average flow under one cm/month by July, except OGI which sustained flow through the dry season.

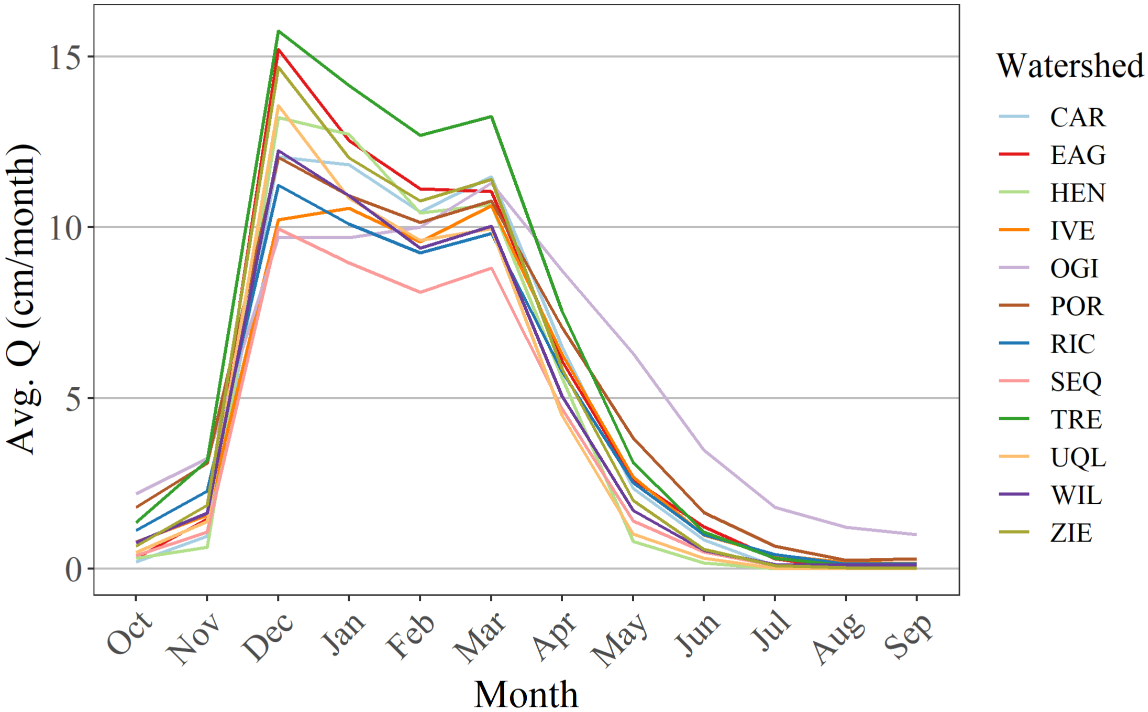

Figure 8. Average monthly streamflow of each stream gage over the hydrologic year, with streamflow generally peaking in December and approaching zero by July with the exception of OGI.

The average annual runoff across the sub-watersheds was 57.7 cm (σ = 31.2 cm) (Figure 9). The minimum annual runoff measured over the study period was 6.9 cm in 2009 at the HEN sub-watershed, however the lowest mean runoff across the sub-watersheds was 18.7 cm (σ = 7.5 cm) in 2014. The EAG sub-watershed had a maximum annual runoff of 157.0 cm in 2003, while the highest mean annual runoff across all sub-watersheds was 120.6 cm (σ = 14.7 cm) in 2006 (Table 5). The sub-watershed with the least amount of variation was SEQ (σ = 25.0 cm), compared to EAG, which had the highest (σ = 39.2 cm).

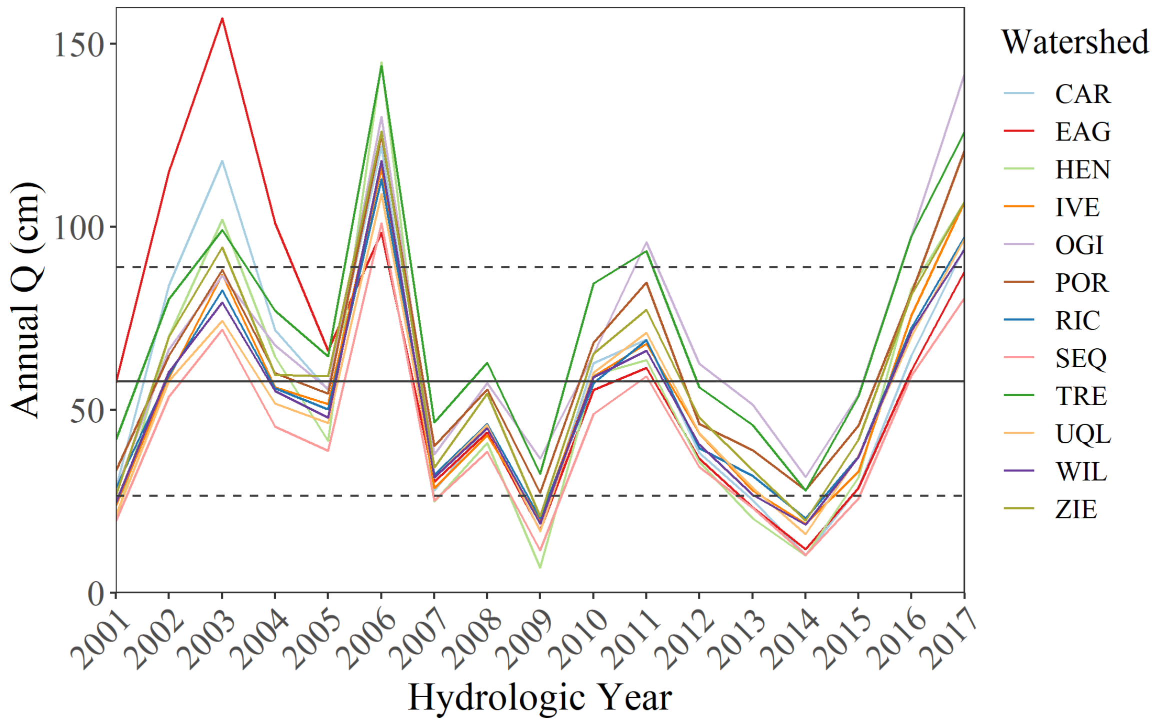

Figure 9. Annual runoff of the headwater sub-watersheds in the CCEW. The record mean and standard deviation across the sub-watersheds are shown by the solid and dashed lines, respectively.

Runoff across the sub-watersheds exhibited a more consistent order compared to the precipitation record, in that the sub-watersheds generally had the same rank from greatest to least runoff across years (Figures 6 and 9). However, this organization did not visually reflect any spatial autocorrelation in the sub-watersheds. An ANOVA demonstrated that there were significant differences between hydrologic years as well as stream gages over the study period ($\alpha = 0.05$).

The monthly streamflow record reflects the precipitation records with wet winters and dry summers (Figure 10). OGI retained streamflow, even when the other sub-watersheds were dry or below their detection limits, particularly in 2009 and 2011 through 2017. As shown in the annual data, EAG had notably higher streamflow, particularly in December early in the study period, but in the second half of the study period was closer to the average streamflow most months.

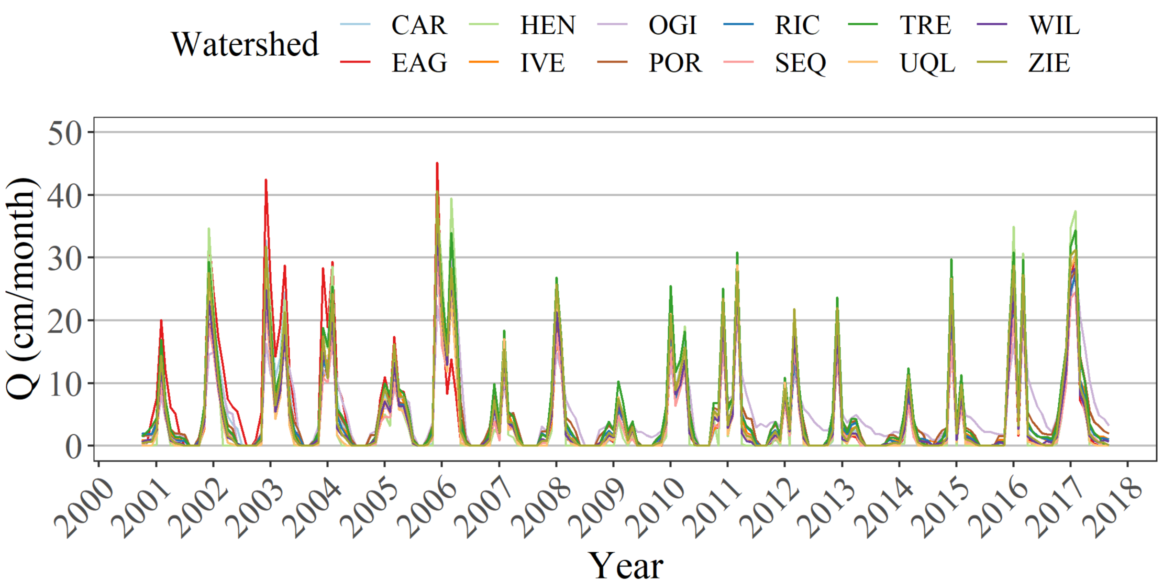

Figure 10. Monthly Q of the sub-watersheds in the CCEW over the study period.

5.1.3 Runoff Ratios

Modified, average monthly runoff ratios ($\overline{RRm}$), as calculated using Equation 3 to eliminate undefined monthly RRs, underlined the variation in the rainfall-runoff relationship among the sub-watersheds across the year (Figure 11). In the winter months, all the sub-watersheds follow a similar pattern — $\overline{RRm}$ increased from a mean of 0.12 in October, peaked around 0.68 in January, then averaged 0.64 from February through April. In January, HEN had the highest $\overline{RRm}$ and SEQ had the lowest (0.88 and 0.49, respectively). After April, the sub-watersheds diverge substantially in response to declining precipitation. OGI, POR, IVE, RIC, EAG, TRE, in that order, had $\overline{RRm}$'s that peak at greater than one in the dry season, indicating streamflow was, on average, greater than precipitation in these months. These sub-watersheds also exhibit an increasing $\overline{RRm}$ in May, a decline in June, and then a sharp rise in July. $\overline{RRm}$ for EAG dropped to zero in August and all except CAR fell below 0.5 by September. A second trend in the dry season was demonstrated by HEN and UQL, where $\overline{RRm}$ decays to zero with no punctuating increases. CAR, SEQ, WIL, and ZIE exhibited intermediate patterns between these extremes.

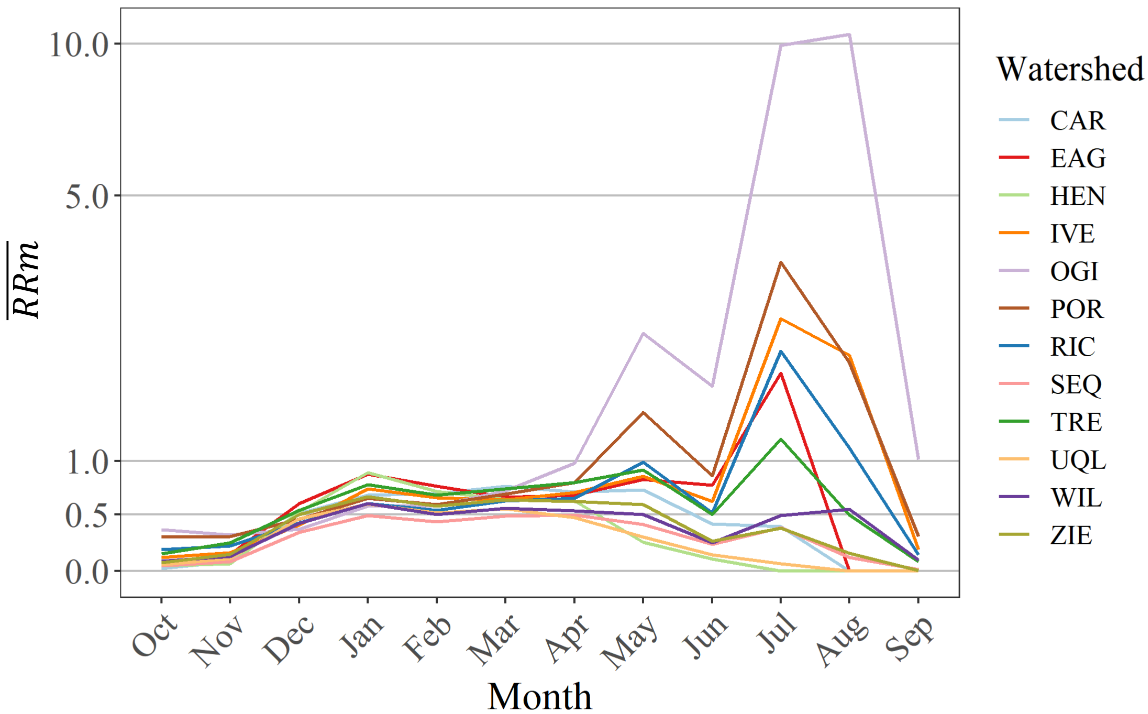

Figure 11. Modified average monthly $\overline{RRm}$ calculated as average Q divided by average P by month, due to substantial numbers of undefined RRs found for individual months. The y-axis is on a log-scale.

The annual runoff ratios across the sub-watersheds had a mean of 0.5 and a standard deviation of 0.2 (Figure 12). The minimum runoff ratio calculated was 0.1 in 2009 in the HEN sub-watershed. That year also had the lowest mean runoff ratio across the sub-watersheds (0.28). The maximum runoff ratio calculated was 1.3 in 2004 in the

EAG sub-watershed, however the highest mean runoff ratio across the sub-watersheds was 0.8 in 2006.

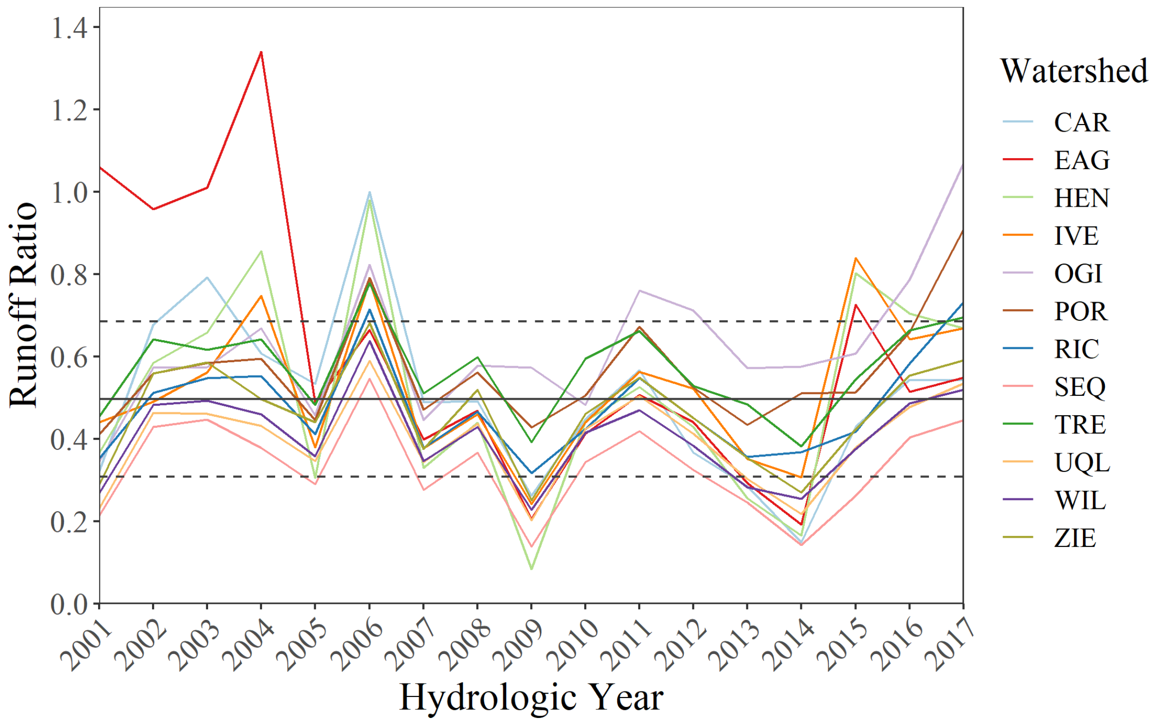

Figure 12. Annual runoff ratios of each sub-watershed. The record mean and standard deviation across the sub-watersheds are shown in solid and dashed lines, respectively.

Monthly runoff ratios over the study period show the greatest variability between the wet and dry season (Figure 13). As demonstrated in the average monthly RR*, monthly RRs in the wet season generally vary from 0.1 to 0.7 and dry season RRs vary more widely, sometime with a value or zero, exceeding 100 or being undefined. Due to the large number of zero and undefined values, this dataset was not used for further analysis.

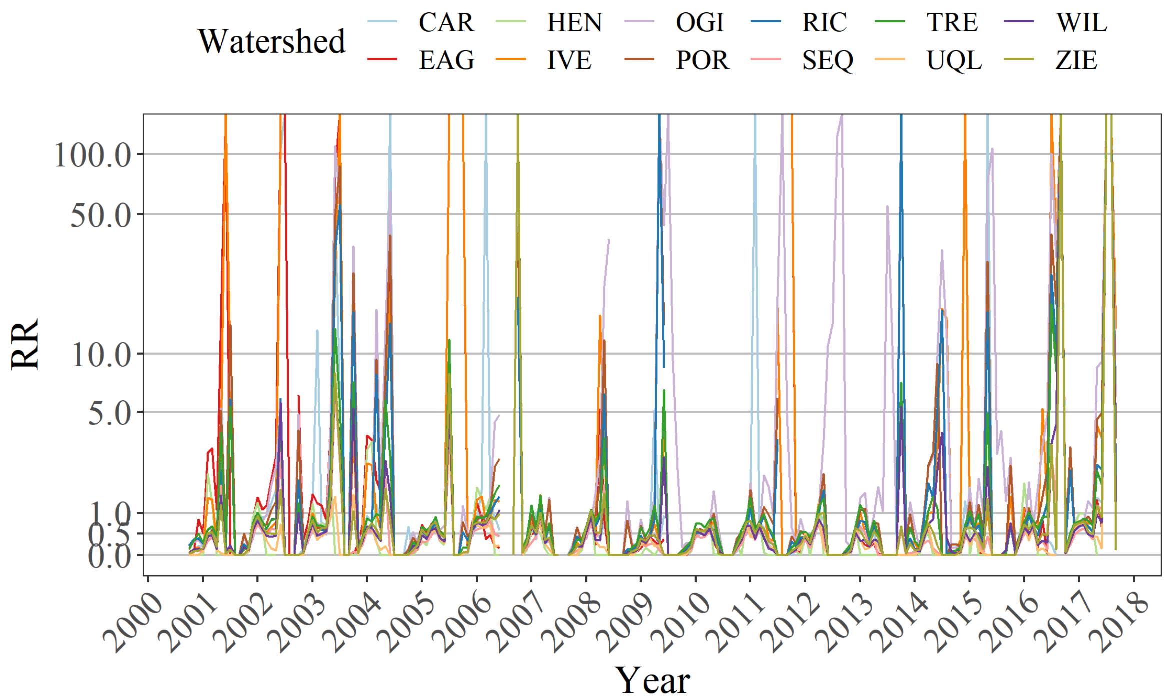

Figure 13. Monthly runoff ratios over the study period. The y-axis is presented in log-scale. 43 months with undefined numbers are not drawn.

5.2 Impacts of Past Precipitation on Streamflow and Runoff Ratios

A lag analysis looking at the impact of past precipitation on streamflow had varying results across timescales, however there was little difference among sub-watersheds (Figure 14). On the annual scale, precipitation was significantly correlated with streamflow for all sub-watersheds at a lag of zero, however lags greater than zero were not significant. The exception was sub-watershed IVE, which had a weak negative correlation between precipitation and streamflow at a 2-year lag. This indicates that past precipitation generally does not influence streamflow on a yearly basis. Seasonal lags ("wet" from December to March and "dry" from June to September) were significant out to six seasons with an oscillation between positive and negative correlations, however there were no substantial decline in the strength of the correlation. All the sub-watersheds were significant at each seasonal lag step. When examining only wet seasons, a similar result to the annual scale emerged, where only present precipitation was significantly correlated with present streamflow. Again, all sub-watersheds were significant. On a monthly scale, lags were significant and positive up to three months but declined in correlation strength. At five and six months, lags were significant with an increasingly negative correlation. All sub-watersheds were significant at each monthly time step except the fourth lag.

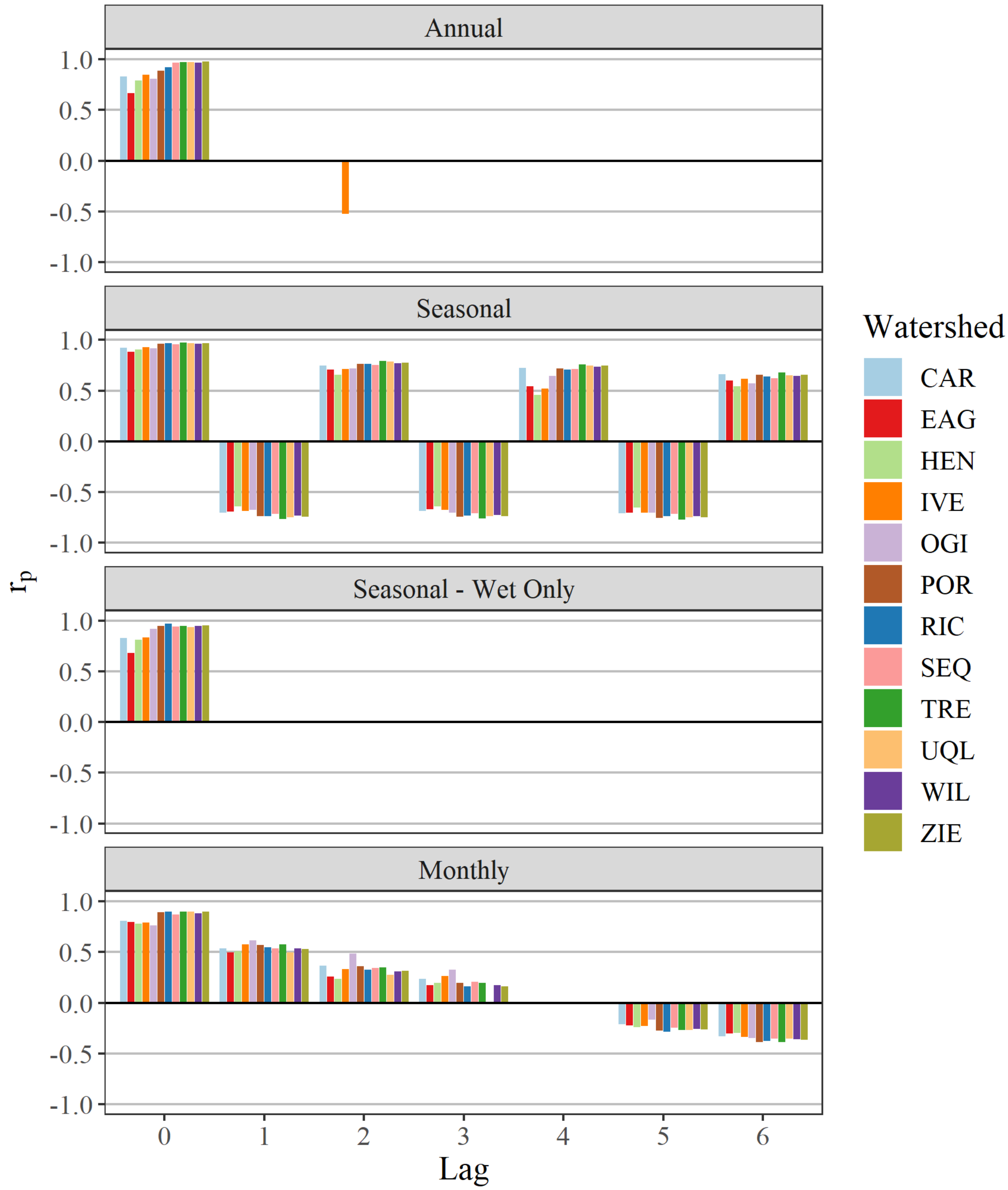

Figure 14. Lag correlation analysis of past precipitation and streamflow at annual, seasonal, wet season only, and monthly time steps from top to bottom. Lag steps (x-axis) represent years (top), seasons (middle panels), and months (bottom). Pearson correlation coefficients (r_p) shown are all significant ($p < 0.05$).

A lag analysis looking at the impact of past precipitation on runoff ratios also had varying results at different timescales, however there was some variation in sub-watersheds (Figure 15). The annual and wet season only timescales had similar results to the streamflow correlation in that only present precipitation was significantly correlated to runoff ratios. However, at the annual timescale, three sub-watersheds (EAG, HEN, and OGI) had no significant lags at any timestep. For the wet season only, three sub-watersheds (CAR, EAG, and HEN) had no significant lags. For the seasonal scale (including dry seasons), lag correlations were significant for some sub-watersheds up to six lags. RIC and TRE had no significant lags. The strength of the correlation appeared to be relatively random over time and by watershed, with UQL having the strongest consistent correlation. Notably, OGI oscillated opposite the other correlation for all except the fifth lag.

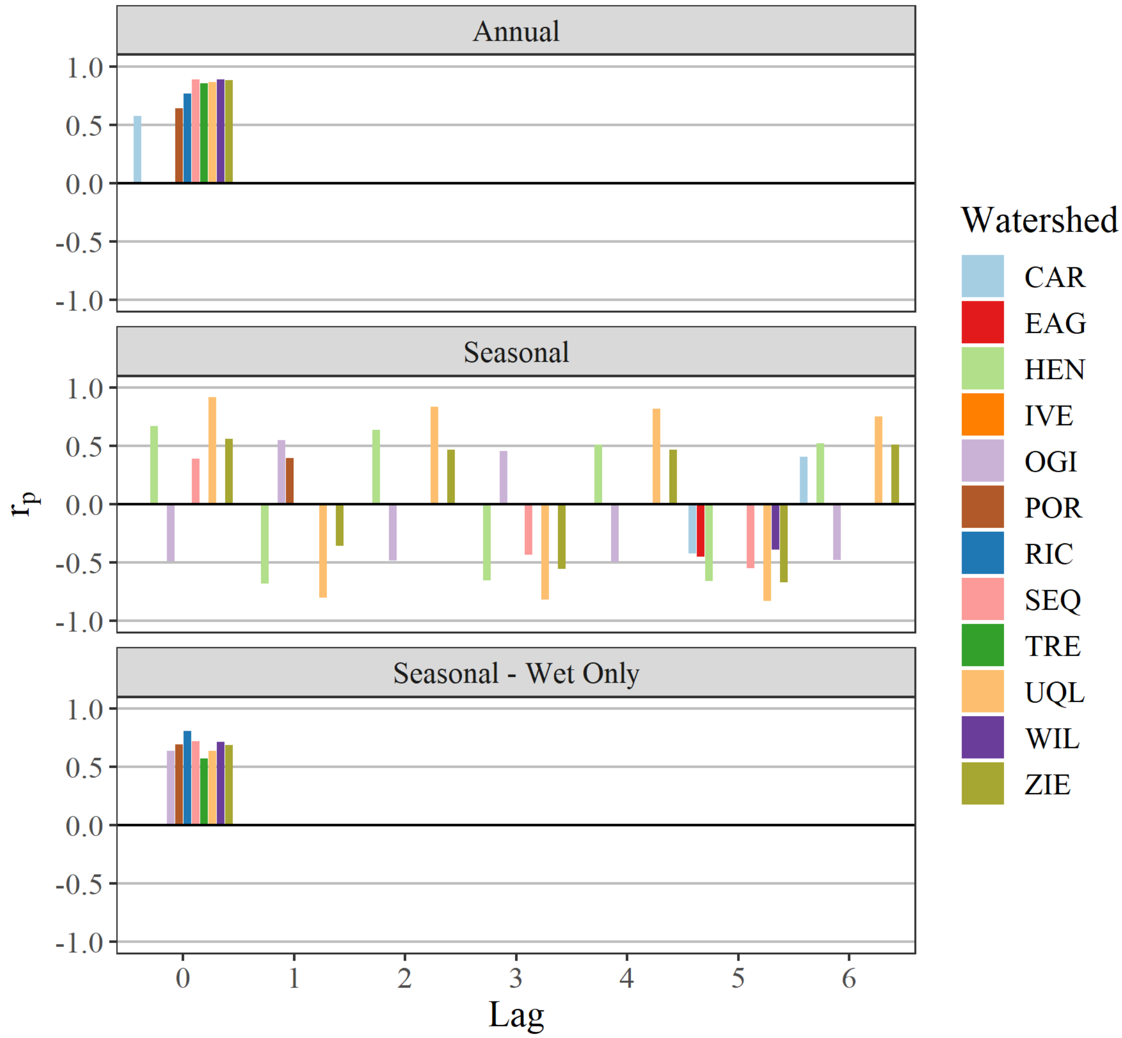

Figure 15. Lag correlation analysis of past precipitation and runoff ratios at annual, seasonal, and wet season only from top to bottom. Lag steps (x-axis) represent years (top), seasons (middle and bottom). Pearson correlation coefficients (r_p) shown are all significant ($\alpha < 0.05$).

5.3 Impacts of Anomalously Dry Annual Precipitation

Four dry years occurred over the seventeen-year study season — 2007, 2009, 2014, and 2015 (Figure 4). Runoff ratios in normal precipitation years were significantly higher on average compared to dry years (Figure 16). The mean runoff ratio in normal years was 0.5 with a standard deviation of 0.2. Dry years had a mean runoff ratio of 0.4

with a standard deviation of 0.2. The normal years had nine anomalously high runoff ratios. Four were from the EAG sub-watershed from 2001-2004, likely driven by high streamflow in those years compared to other sub-watersheds (Figure 9). The remainder were from HEN in 2004 and 2006, CAR in 2006, OGI in 2017, and POR in 2017. There were two anomalously high runoff ratios in the dry years from 2015 in the HEN and IVE sub-watersheds.

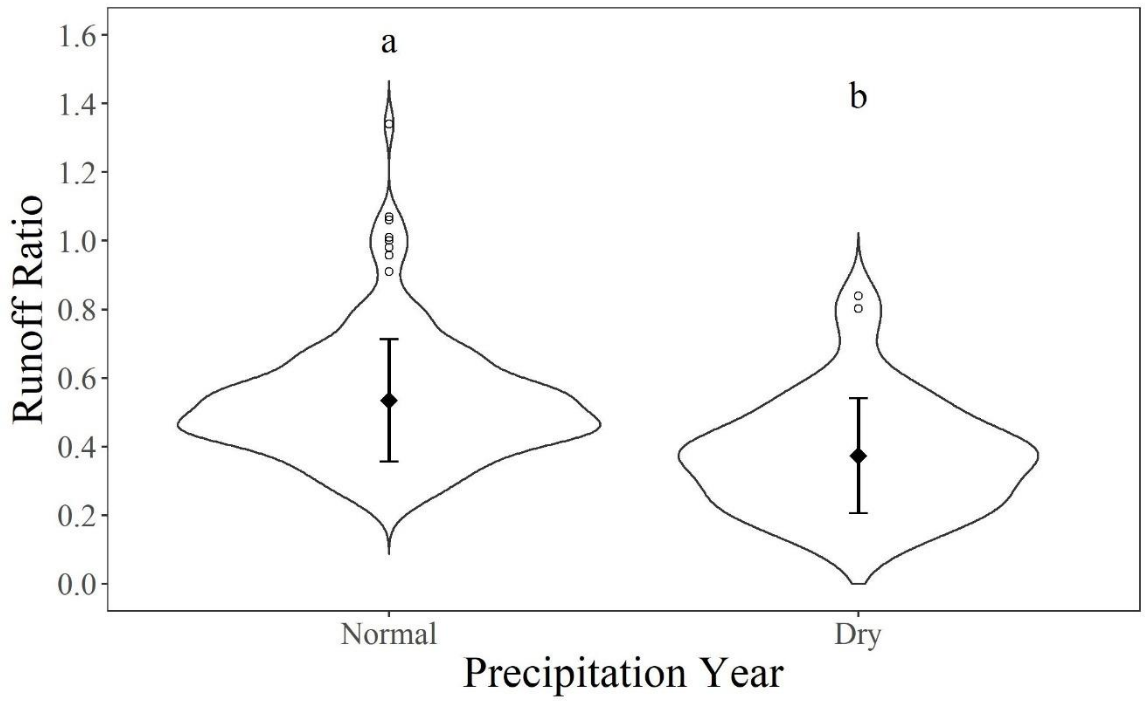

Figure 16. The distribution of annual runoff ratios in normal versus dry precipitation years. A Tukey HSD test found that normal years had a significantly greater mean runoff ratio as compared to dry years.

5.4 Effects of Watershed Properties on Runoff Ratios

Out of the ten variables tested for describing differences in watershed property effects on runoff ratios using ANOVA (Table 4), three were found to be significant: mean aspect, SDI, and mean soil depth ($p = 0.05$). Watershed area, mean elevation,

elevation range, mean slope, mean TWI, mean BA, and harvest disturbance were not significant predictors of runoff ratios.

North-facing sub-watersheds had significantly higher mean runoff ratios than west- and south-facing sub-watersheds (Figure 17). North-facing sub-watersheds had a mean annual runoff ratio of 0.6 while west- and south-facing sub-watersheds both had means of 0.5. There was also less variability in the runoff ratios of the north-facing sub-watersheds ($\sigma = 0.1$) compared to the west- and south-facing sub-watersheds ($\sigma = 0.2$). All three distributions were relatively normal with slight skews towards lower runoff ratios. The west-facing sub-watersheds in particular had several outliers with runoff ratios ranging from 1.0 to 1.3.

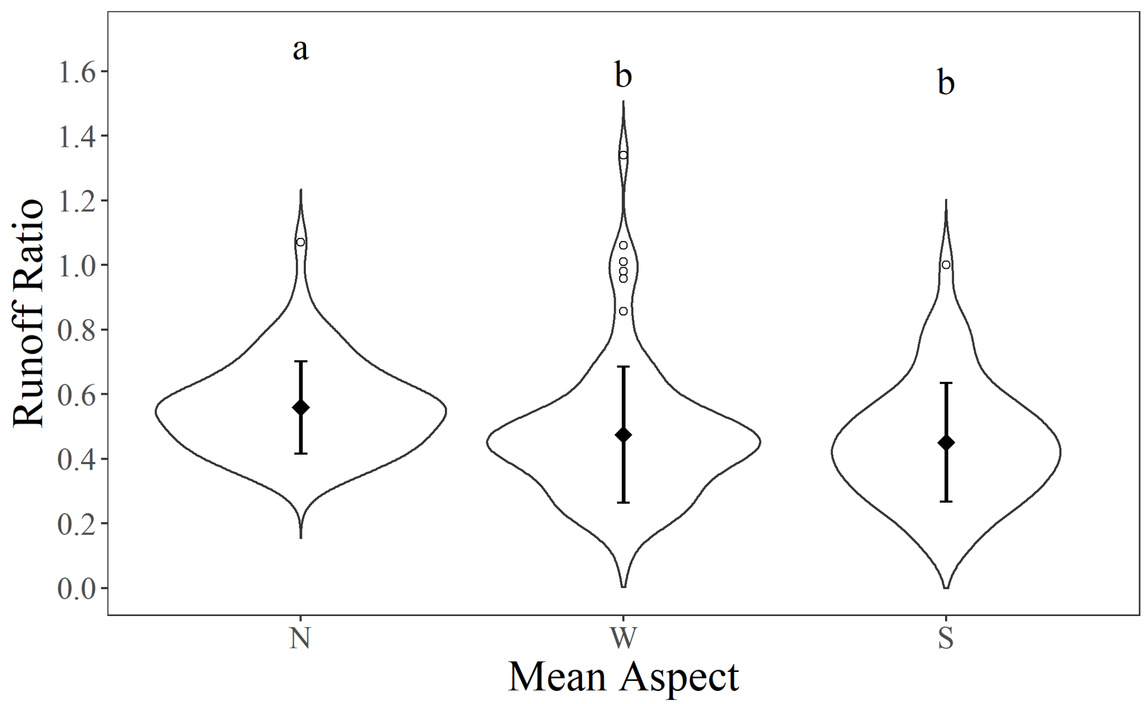

Figure 17. The distributions of runoff ratios for north-, west-, and south-facing sub-watersheds. The mean runoff ratios for each aspect are symbolized by the black diamonds with standard deviation bars. Outliers are shown as hollow circles. A Tukey HSD test found sub-watersheds with a north-facing mean aspect had significantly higher runoff ratios than west and south facing sub-watersheds, indicated by a and b groups.

Mean runoff ratios for low SDI sub-watersheds were significantly higher than high SDI sub-watersheds, with mid SDI sub-watersheds not being significantly different from high or low sub-watersheds (Figure 18). Sub-watersheds with low SDI had a mean runoff ratio of 0.55 compared to 0.51 for mid SDI and 0.46 for high SDI sub-watersheds. Runoff ratios for low SDI sub-watersheds had a high variability (σ = 0.27), while mid and high SDI sub-watersheds had relatively smaller standard deviations for their runoff ratios (σ = 0.16 and 0.17, respectively). The distribution of the runoff ratios for the mid and high SDI sub-watersheds was relatively normal, while the low SDI sub-watersheds had a greater positive skew.

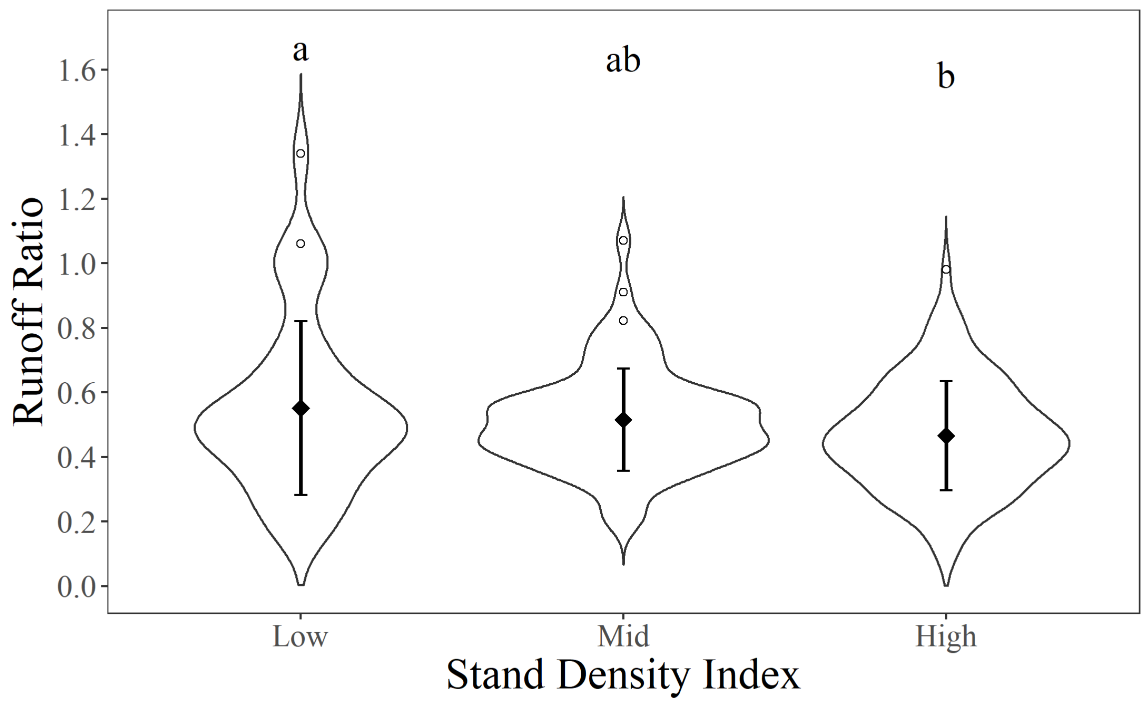

Figure 18. The distributions of runoff ratios for low, mid, and high SDI sub-watersheds. The mean runoff ratios for each are symbolized by the black diamonds with standard deviation bars. Outliers are shown as hollow circles. A Tukey HSD test found sub-watersheds with a low SDI had significantly higher runoff ratios than high SDI sub-watersheds, indicated by a and b groups. Mid SDI sub-watersheds were intermediate between high or low SDI sub-watersheds.

Mean runoff ratios were significantly lower for sub-watersheds with shallow soil depths (low), compared to those with deeper soils (mid and high; Figure 19). Sub-watersheds with the shallowest soils had a mean runoff ratio of 0.42 ($\sigma = 0.11$). Mid soil depth sub-watersheds had a mean runoff ratio of 0.53 ($\sigma = 0.22$), while high soil depth sub-watersheds had a mean of 0.50 ($\sigma = 0.17$). Mid and high soil depths sub-watersheds also had notably greater variability in runoff ratios with positive skews as compared to the sub-watersheds with shallower soils.

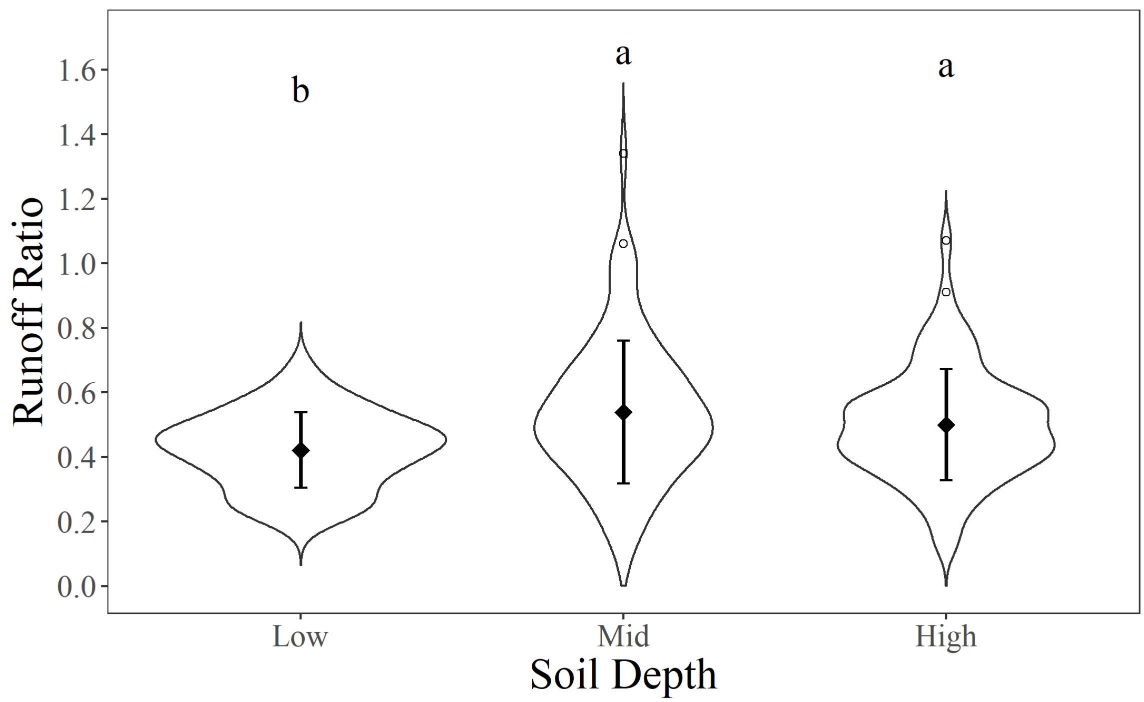

Figure 19. The distributions of runoff ratios for low, mid, and high soil depth sub-watersheds. The mean runoff ratios for each are symbolized by the black diamonds with standard deviation bars. Outliers are shown as hollow circles. A Tukey HSD test found sub-watersheds with a low or shallow soil depth had significantly lower runoff ratios than sub-watersheds with deeper soils (mid and high), indicated by a and b groups.

An AIC test comparing the three significant watershed properties determined that soil depth was the best-fit model to explain variability in annual runoff ratios, with an

AICc weight of 60% (Table 6). This was followed by aspect, which together with soil depth, had a cumulative weight of 98%. This indicates that soil depth and aspect together make up 98% of the predictive power of the model.

Table 6. AIC output to best explain variability in annual runoff ratios.

Watershed Property	K	AICc	Delta AICc	AICc Weight	Cumulative Weight	Log Likelihood
Soil Depth	4	-107.38	0	0.6	0.6	57.79
Aspect	4	-106.45	0.92	0.38	0.98	57.33
SDI	4	-100.92	6.46	0.02	1	54.56

5.5 Combined Effects of Drought and Watershed Properties

A two-way ANOVA model using precipitation anomaly and aspect determined that all aspects in normal years had significantly higher runoff ratios compared to west- and south-facing sub-watersheds in dry years (Figure 20). North-facing sub-watersheds in dry years were intermediate, without a significant difference in runoff ratios between either grouping.

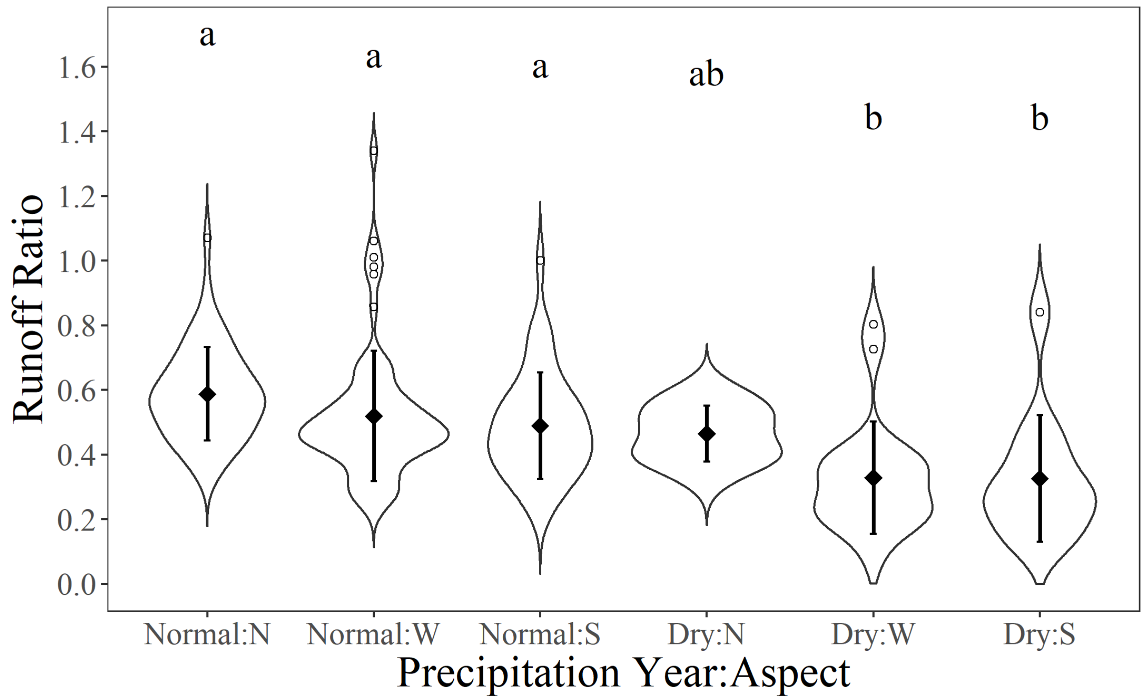

Figure 20. The distribution of runoff ratios when examining the interaction between anomalous precipitation years and sub-watershed aspect.

A two-way model using precipitation anomaly and SDI produced more intermediate groupings with little clear effect from SDI (Figure 21). The low and high bins were both significantly different between normal and dry years, while the mid bin has no difference between normal and dry years. Additionally, the mid and high bins in normal years and the low and mid bins in dry years had no significant difference.

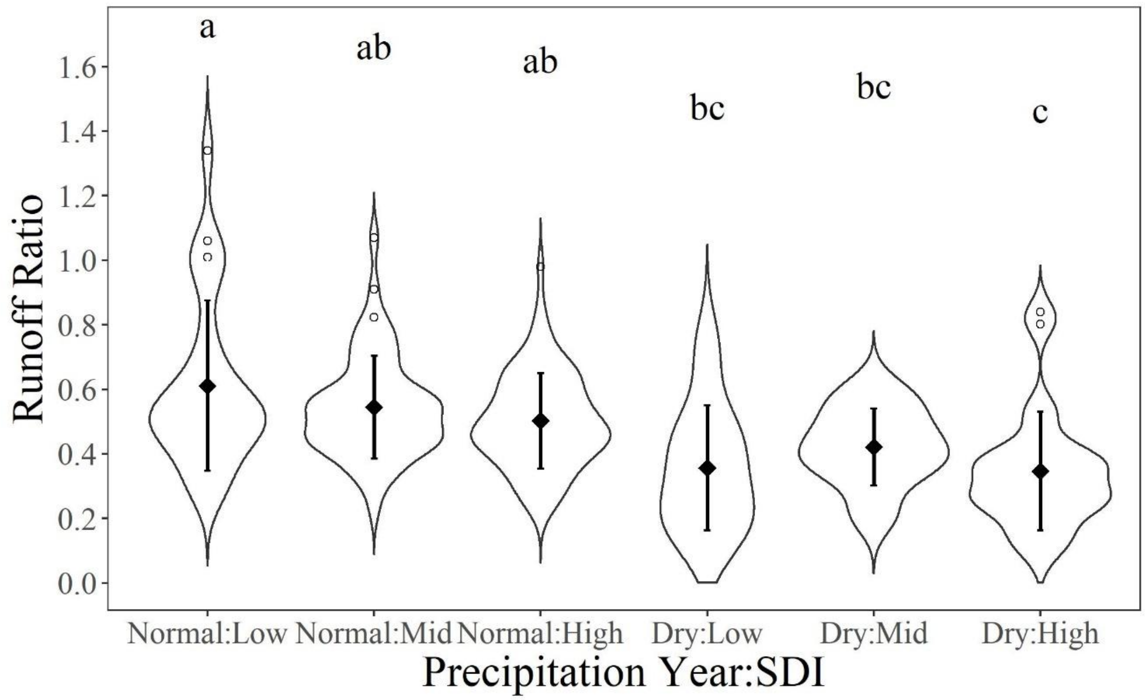

Figure 21. The distribution of runoff ratios when examining the interaction between anomalous precipitation years and SDI.

A two-way model between precipitation anomaly and soil depth showed that shallow (low) and mid depth soils were significantly different between dry and normal years (Figure 22). In contrast, deeper soils (high) were not significantly different between dry and normal years. This result shows that deeper soils exhibit a more moderate shift in runoff ratios in anomalously dry years.

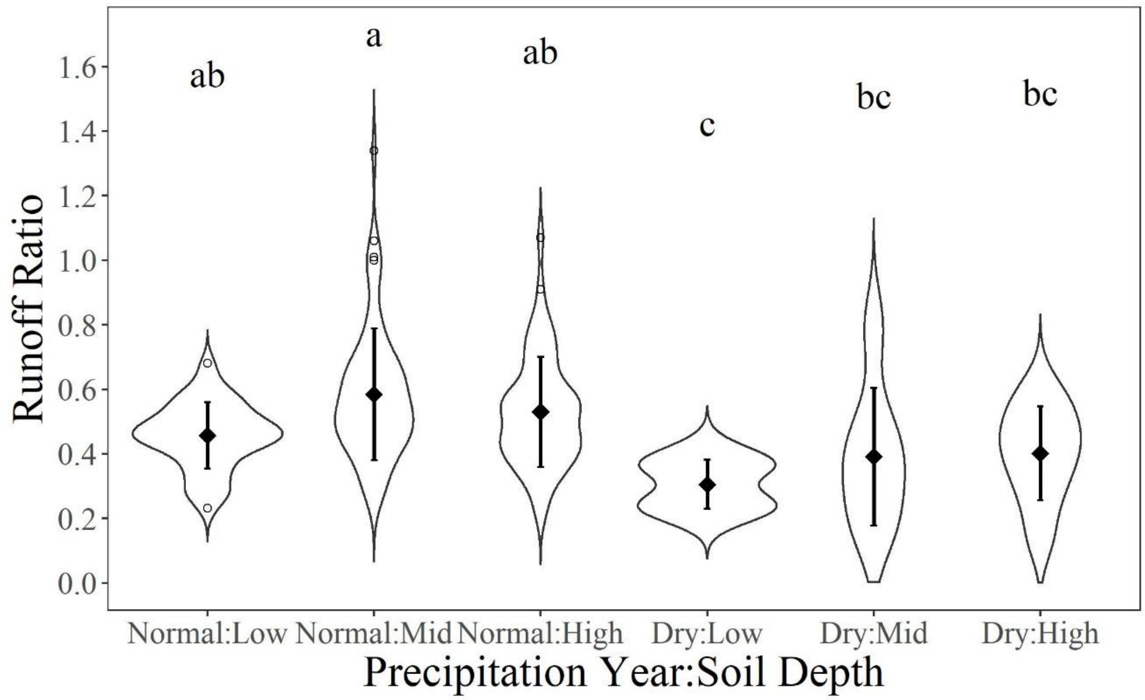

Figure 22. The distribution of runoff ratios when examining the interaction between anomalous precipitation years and soil depth.

Results from two-way ANOVAs between precipitation anomaly and significant watershed properties indicate that combined models are a better fit than those with only one independent variable (

Table 7). Additionally, combined models with precipitation anomaly and a significant watershed property were found to be better fit models than either single variable. Although all combined models tested were found to be significant, when two-way models were constructed with an interaction variable, the interaction was not found to be significant.

Table 7. AIC results comparing all significant ANOVA models for annual runoff ratios.

Watershed Property	K	AICc	Delta AICc	AICc Weight	Cumulative Weight	Log Likelihood
P Anom.:Soil Depth	5	-136.24	0	0.62	0.62	73.27
P Anom.:Aspect	5	-135.16	1.08	0.36	0.98	72.73
P Anom.:SDI	5	-128.74	7.5	0.01	1	69.52
P Anom.	3	-125.52	10.72	0	1	65.82
Soil Depth	4	-107.38	28.86	0	1	57.79
Aspect	4	-106.45	29.78	0	1	57.33
SDI	4	-100.92	35.32	0	1	54.56

6. DISCUSSION

6.1 Hydroclimate Trends and Runoff Ratio Utility

The CCEW has been the focus of hydrologic study for more than six decades, beginning as a paired watershed study and shifting to examine processes at the sub-watershed scale. By 2001, streamflow in the North Fork sub-watersheds was showing signs of recovery after harvest in the second experiment, and sub-watersheds in the South Fork were gauged in anticipation for a third experimental harvest (Keppeler et al., 2003). This study utilizes data from 2001 – 2017 in the South Fork CCEW, which was a period of low disturbance on the landscape. The high density of rain and stream gages allowed me to test the temporal and spatial controls on the rainfall-runoff relationship in the sub-watersheds of the CCEW.

During the data exploration phase, I found that average annual precipitation over the study period was 4% lower than the long-term average annual precipitation (1963-2022), and there was no significant trend in annual precipitation from 2001-2017. Keppeler et al. (2024) found a similar pattern in the CCEW with no significant trend in long-term annual precipitation, but a 6% difference in precipitation between the 1962-1984 second experiment reference period and 1985 to 2022. This lack of significant trend matches other analyses, which find precipitation in California is changing more significantly in timing and intensity rather than annual totals (Li and Ding, 2024; Lukovic et al., 2021).

Annual streamflow for all the sub-watersheds also did not exhibit a significant trend over the study period, with the exception of EAG (Figure 9). The significance of this trend appears to be driven largely by higher-than-average annual streamflow from 2001-2004. This was hypothesized to be due to a rating curve error associated with equipment replaced in 2004 (Liz Keppeler, personal communication, May 6, 2022). However, it is more likely that this is a response to post-harvest thinning in conducted in 2001, which removed 75% of the basal area (Keppeler et al., 2024). Increased water yields were observed for about 10 years after treatment for the first and second experiments at the CCEW (Keppeler et al., 2008). The CAR sub-watershed was also thinned in 2001, and it has the second highest streamflow from 2002-2004. However, it is not an outlier to the same magnitude as EAG, indicating that response to thinning can vary.

These outlier years are even more evident in the RR time series where EAG has an annual RR greater than 1 in three of the four outlier years (Figure 12). Only three other sub-watersheds had an annual RR greater than one (HEN and CAR in 2006 and OGI in 2017). An RR greater than one implies that the watershed received less precipitation than was produced in streamflow, an efficiency not well explained by the traditional water balance equation (Equation 2). At the annual timescale, this could be explained in numerous ways. First, the precipitation at the nearest rain gage may be an underestimation of the precipitation received over the entire sub-watershed area, resulting in an artificially high RR. Such a possibility was suggested by Saksa, et al. (2017) when the combined annual Q and predicted actual ET consistently exceeded P at CCEW from 2004 to 2015. Another possibility could be an underestimation of precipitation due to instrument error challenges at CCEW. As a general rule, nearby objects should be twice their height in distance away from a rain gage to prevent wind field effects (World Meteorological Organization, 2008). Coastal redwoods, as well as other native conifers, commonly reach heights in excess of 100 meters, presenting interception problems that may interfere with accurate rain gage totals. Utilizing a spatial precipitation model such as PRISM could aid in addressing these potential issues (PRISM Climate Group, 2017). An alternative explanation may be that watershed storage carried over from the previous year could supplement streamflow, as was observed in Nippgen et al. (2016) where annual RRs had similar correlation strengths with the current and previous year's precipitation. However, this "watershed memory" would have to account for a substantial portion of streamflow to reach an RR of one or greater. Previous research at the CCEW found that over 20 percent of annual precipitation was intercepted and evaporated off the forest canopy alone (Reid and Lewis, 2009). Watershed storage would have to make up for the full loss of water to evapotranspiration in order to equate streamflow to precipitation which could consist of over a fifth of the water budget. Given that the characteristics that determine watershed storage (soil type, depth, underlying geology, etc.) do not change on interannual timescales, we should also expect watershed storage contributions show consistency across our study period. These outlier RRs observed in the EAG sub-watershed disappear after 2004, indicating a more temporally acute explanation is appropriate. Despite these outliers, the annual RRs in the study had a mean of 0.5. Annual RRs observed in regional studies of coastal Pacific Northwest watersheds have ranged from 0.49 to 0.96 (Chang et al., 2014), 0.45 to 0.92 (Asarian and Walker, 2016), and greater than 0.40 (McCabe and Wolock, 2016). Other comparable experimental watersheds in the region report similar RRs such as 0.55 at the H. J. Andrews Experimental Forest 0.53 at Coyote Creek Experimental Forest (Jones and Post, 2004) and 0.65 at Elder Creek in the Angelo Coast Range Reserve, (Salve et al., 2012).

The contrast across watersheds is made more stark utilizing the $\overline{RRm}$ (Figure 11). The $\overline{RRm}$ demonstrated a pronounced divergence in the monthly rainfall-runoff relationship across sub-watersheds, particularly in the early dry season. The cause of this divergence is not immediately obvious, however watersheds with higher dry season $\overline{RRm}$ tend to have deeper soils. This indicates that the water storage capacity of the sub-watershed plays an increasingly important role in streamflow generation as precipitation declines. Soil depth in combination with the deeper subsurface critical zone structure of the Franciscan Complex, where CCEW is situated, has been shown to be a significant control on dry season streamflow generation (Hahm et al., 2019). The influence of soils on RRs will be examined later in this discussion.

6.2 Short-Term Memory of Caspar Creek Headwaters

This project set out to better understand the hydrologic resilience of North Coast headwater streams by examining the impact of past precipitation on the streamflow and runoff ratios of the CCEW at annual, seasonal, and monthly timescales. Precipitation was significantly correlated with streamflow at a lag of zero for the annual and wet season only timescales (Figure 14). At the annual scale, eight of the twelve sub-watersheds had a significant correlation with precipitation at zero lags, however there was no significant correlation in lags beyond that point. A similar result was seen in the wet season only analysis.

The seasonal analysis, which included the dry season, found that streamflow had significant correlations out to six lags which oscillated between positive correlations in even-numbered lags and negative correlations in odd-numbered lags. The correlation strength did not show a substantial decline, indicating that the significance of this result is likely due to autocorrelation in the seasonal streamflow dataset and not an indication of past precipitation's influence on streamflow. The seasonal analysis using runoff ratios featured a more perplexing result. Three sub-watersheds, HEN, UQL, and ZIE, showed the same oscillating pattern seen in the streamflow analysis. One sub-watershed, OGI, showed an opposite pattern with positive correlations in odd-numbered lags and negative correlations in even-numbered lags. Additionally, SEQ, POR, CAR, EAG, and WIL all had at least one significant lag result, though these results appeared random. In all, the lag-correlations between season precipitation and runoff ratios presented no discernable pattern across the sub-watersheds. This result may be due to an abundance of zeroes in the runoff ratio dataset due to the dry season, skewing the data in a non-normal distribution. Given this, dependence at seasonal timescales may not be revealed using the Pearson correlation coefficient which assumes a normal distribution. Though the assumption of normality is fairly robust to nonconformity, a non-parametric statistic such as the Spearman's rank correlation coefficient may be more appropriate (Hao and Singh, 2016; Härdie et al., 1997; Rahman et al., 2017). The rainfall-runoff relationship also exhibits non-linearity as rainfall declines and the Spearman correlation is less sensitive to outliers due to being a rank correlation. The tail dependence coefficient, which tests for dependence in the extremes of a dataset, could help tease out questions surrounding seasonal extremes, drought, and watershed memory (Frahm et al., 2005; Hao and Singh, 2016).

On the monthly scale, lags were significant and positive up to three months but declined in correlation strength, without a notable difference across sub-watersheds. This three-month lag corresponds with the observed declines in streamflow over the dry season. The average monthly streamflow of the sub-watersheds is near zero by August, three months after precipitation declines substantially in May. This would indicate that the watershed memory of the headwater sub-watersheds of the CCEW are a maximum of three months.

As a relatively new concept, watershed memory is loosely defined, with various metrics in use to detect its existence. These recent work of Keppeler et al. (2024) at CCEW used a persistence metric, defined as the number of months after the end of a drought for which the Standardized Runoff Index (SRI) was less than the Standardized Precipitation Index (SPI), to test the question of watershed memory. The persistence metric indicated that streamflow drought can persist anywhere from 1 to 19 months after the end of meteorological drought in the North and South Forks of CCEW. This is a different conception of watershed memory which is dependent on a drought event framework as compared to my time series correlation. Though my results indicate that past precipitation only influences streamflow on monthly timescales, Keppeler et al. (2024) demonstrates that drought can still have lasting effects on watershed hydrology. In addition, these studies examined watersheds at different spatial scales, indicating that cumulative effects should be considered when investigating watershed memory.

The sub-watersheds at CCEW do not have a watershed memory that carries over from year-to-year, which contrasts with findings from the Coweeta watershed (e.g., Nippgen et al., 2016). Compared to CCEW, where approximately 90% of rainfall occurs between October and April, rainfall at Coweeta is relatively even throughout the year with only a slight increase in the winter months (10-14%) (Swift Jr et al., 1988), ensuring that runoff ratio values will always be defined numbers. This climate also ensures that the water storage at Coweeta is constantly being replenished, thus leading to perennial streamflow. In comparison, the dry season at CCEW appears to be longer than the time necessary to fully "drain" the water storage in the headwater streams, resulting in flow reaching zero in most sub-watersheds in most years. Due to the annual dry season at CCEW, the monthly dataset featured an abundance of months with zero measurable precipitation or streamflow, which resulted in 43 months with an undefined RR and 556 months with an RR of zero. Due to this, the monthly RRs could not be used for a lag correlation analysis.

6.3 The Small, but Significant Effects of Watershed Properties

At first glance, the landscape of the CCEW can appear homogenous. All the watersheds feature a mixed conifer forest growing on steep topography within the same geologic unit and similar soils. Stark differences in ecology, driven by aspect, solar exposure, and rain shadows are not observed as they are in more continental climates

(Yetemen et al., 2015). Due to this homogeneity, the sub-watersheds of the CCEW are utilized as replicates to test the effects of forest harvest practices on watershed processes. This analysis does not upend this presumption, but it does introduce several caveats to be considered in future studies on the rainfall-runoff relationship.

An ANOVA of the annual RRs of each sub-watershed over the study period indicated that there were significant differences between the sub-watersheds that had yet to be explained. The results of the ANOVAs testing the correlation between various watershed properties and runoff ratios indicated that watershed aspect, SDI, and soil depth were significant variables.

In regard to aspect, north-facing sub-watersheds had a mean RR that was 18% higher than south- and west-facing sub-watersheds. In addition, the standard deviation of the north-facing sub-watershed's RRs was half that of the west- and south-facing sub-watersheds. This observation of greater annual RRs with less variation in north-facing watersheds is most likely due to decreased solar radiation on these sub-watersheds, leading to lower ET rates which would allow more water to reach the stream. This observation is somewhat unexpected, as aspect does not appear to be a driver of differences in the vegetative community in the CCEW, a classic indicator of water availability (Desta et al., 2004). This result would imply that water lost to evapotranspiration is great enough to influence streamflow generation, but not great enough to change the vegetative landscape, as seen in more arid environments (Holland and Steyn, 1975).

Fog cover was also hypothesized to temper the effects of aspect as it is common year-round, despite the stark differences in wet and dry seasons in terms of precipitation (Chung et al., 2017; Petreshen et al., 2025). Hypothetically, fog cover could diffuse direct solar radiation, tampering its effect, while also supplementing transpiration through foliar uptake. Despite this hypothesis, these results indicate that aspect is still an influential factor on runoff ratios, though interactions with fog should be explored in future studies.

Aspect was the only topographic variable tested with significant differences in RRs across the sub-watersheds. This contrasts with an investigation into controls on subsurface flow variability which found that aspect explained over ten percent of the water table response, however other topographic variables such as slope and profile curvature had greater explanatory power (Bachmair and Weiler, 2012). Nippgen et al., (2016) found no effect from aspect on RRs at Coweeta Hydrological Laboratory's marine, humid temperate climate, but there was a strong positive effect from elevation. Meanwhile, another study at Coweeta found post-harvest streamflow recovery occurred at a faster rate in south-facing stands compared to north-facing stands (Ford et al., 2011). These differing results indicate the importance of context when evaluating the effects of watershed characteristics on hydrologic response variables. Patterns observed in the water table at a hillslope scale may not necessarily be observed in streamflow response at the watershed scale.

Of the forestry variables tested, SDI was the only one which produced a significant trend in RRs across the groups. Sub-watersheds with low SDI (330-430) had significantly greater RRs compared to sub-watersheds with high SDI (530-630), while mid SDI sub-watersheds (430-530) did not have significantly different RRs from high or low SDI sub-watersheds. The low SDI sub-watersheds likely had greater RRs due to decreased transpiration rates from the lower density forest stands and increased interception loss in high SDI sub-watersheds (Coble et al., 2020). Flux tower experiments have found that ecosystem ET positively correlates with stand age (Jassal et al., 2009). The lower SDI watersheds were clearcut in the second CCEW experiment in 1991 and thus represent younger, even aged-stands which have undergone native forest succession (Richardson et al., 2021). Analysis of the first two experiments at CCEW has found that annual streamflow in the North and South Fork watershed increased by fifteen percent for between eight and eleven years after harvest before returning to preharvest levels (Keppeler, 1998). However, this result indicates that the effects of harvest within the sub-watersheds correlates to an extended change in the rainfall-runoff relationship as compared to the larger watersheds (Ford et al., 2011; Jones and Post, 2004; Perry and Jones, 2016). Despite greater RR's, the low SDI sub-watersheds had a higher variability in RR's than either mid or high SDI sub-watersheds. Low density stands may be more vulnerable to interannual variability, as canopy gaps allow greater exposure to wind and solar radiation and decrease the rate of canopy interception (O'Hara et al., 2017). Younger trees have less developed root systems and tend to be less efficient with water use, resulting in greater drought stress (Ford et al., 2011; Jones et al., 2022; Kwon et al., 2018). In addition, understory plants are generally more sensitive to fluctuations in water variability and low density stands typically have greater understory density (Lechuga et al., 2017). Cumulatively, these factors could explain the greater variability in RR's observed in the low SDI sub-watersheds. Altogether, these results indicate that timber harvest can increase streamflow production in headwater catchments but may also prolong the ecosystem's sensitivity to hydroclimate variability as compared to the larger watershed. This implies that watershed scale and timescale should be considered when evaluating potential impacts from timber harvest.

An interesting feature of the SDI grouping is that they do not completely correlate with the sub-watershed harvest nor BA (Table 2; Table 4). Several sub-watersheds harvested in Experiment 1 have SDIs equal to or exceeding the SDI of control sub-watersheds that were last harvested before 1900. This highlights the need to explore an assortment of forest statistics when assessing harvest effects on watershed processes rather than assume one may be a proxy for all.

Although there are eight different soil complexes mapped in the sub-watersheds, all the sub-watersheds on average have a clay loam texture, with the exception of OGI, which has a sandy clay loam texture. However, soil depth, which ranged from 109.1 cm to 141.7 cm on average, was found to have a significant influence on RRs. Shallow soils (109-118 cm) had significantly lower RRs compared to mid and deep soils (118-130 and 130-142, respectively). This represented a 23% difference in RRs between shallow and mid-depth soils and a 17% percent difference between shallow and deep soils. Soil depth is a key determinant of soil water storage and shallower soils will hold the water table closer to the surface, while also reducing the depth of the unsaturated zone (Hewlett and Hibbert, 1967; Rodriguez-Iturbe et al., 2007). Shallower soils may have reduced RRs due to a greater susceptibility to ET as soil water is held closer to the surface, while deeper soils have been shown to facilitate subsurface flow (Bachmair and Weiler, 2012). Deeper soils hypothetically could protect soil water from uptake through plant roots, however the soil depths mapped within the CCEW are all within accepted rooting depths for coast redwood and Douglas-fir (Flint et al., 2024). Interestingly, shallow soils exhibited almost half as much variability in RRs compared to mid and deep soils, a result opposite of what was expected. A recent analysis on hillslope moisture dynamics at the CCEW found that deeper soils were at times more responsive to rain events and had overall greater variability in moisture than shallower soils (Dymond et al., 2021b). Preferential pathways along with relatively sandy soils at all depths were likely explanations for this phenomenon. Another study with a curious finding includes an analysis of rainfall-runoff shifts during drought, in which soil depth was found to correlate with a downward shift in the runoff coefficient, indicating that deeper soils may partition more water to storage relative to streamflow, such that interannual variability in precipitation causes deeper soiled watersheds to be more variable in streamflow generation (Saft et al., 2016). Connections between soil characteristics, moisture dynamics, and runoff generation warrant further investigation at the CCEW. Soil depth may also explain variability observed in the dry season in the $\overline{RRm}$ time series. Six sub-watersheds (EAG, IVE, OGI, POR, RIC, and TRE) had a July $\overline{RRm}$ greater than one. These sub-watersheds make up two-thirds of the mid and deep soil sub-watersheds, indicating a strong, positive relationship between $\overline{RRm}$ and soil depth in the dry season. This correlation signals the potential utility of the $\overline{RRm}$, which could be examined in future analyses.

In the average monthly streamflow, OGI was an outlier, retaining flow throughout the dry season. As noted above, it is also the only sub-watershed with a sandy clay loam texture compared to the clay loam texture of the other sub-watersheds. However, a sandier soil generally has a lower porosity, allowing for less water storage. An alternate explanation for OGI's exceptional retention of streamflow may be due to the fact that OGI is the only sub-watershed with private residences within its boundary. LiDAR derived DEMs indicate the presence of ponds, which could retain water, reducing streamflow in the wet season. Satellite imagery shows the presence of lawns, which if irrigated in the summer, could subsequently supplement streamflow in the dry season. If these activities are present on the landscape, the scale of their impacts, if any, need to be accounted for in any analysis involving the OGI watershed.

6.4 Drought Interactions

In the analysis examining RRs between dry years and normal years, the ratio of P partitioning to Q was significantly less in dry years (Figure 19). During drought, the overall surface area of the watershed, which is a major determinant of the evaporation rate, has not changed, thus we can expect that the rate at which rainfall is lost to evaporation to be relatively constant or perhaps even increase if the drought is associated with higher-than-average temperatures. The results of the two-way ANOVA testing the interaction between drought status versus aspect showed north-facing sub-watersheds in the dry years had RRs that were intermediate between the normal years and west- and south-facing sub-watersheds in the dry years (Figure 20). Using aspect as a proxy for incident solar radiation, lower solar exposure (north-facing aspect) provides some resilience to the rainfall-runoff relationship of a sub-watershed during a dry year.

The two-way ANOVA between drought status and SDI produced no clear effect (Figure 21). Though it may be expected that water-stressed plants would seek to use whatever water is available, there is evidence of ecosystem-scale resilience to drought in the form of increased water-use efficiency (Ponce Campos et al., 2013). However, laboratory experiments have demonstrated that *S. sempervirens* maintained high transpiration rates relative to its cousin *Sequoiadendron giganteum* (Lindl.) Buchh. (giant sequoia) under drought conditions (Ambrose et al., 2015). Recent work in the CCEW has indicated that timber harvest has been both observed to shorten and reduced two streamflow droughts in 1977 and 2021, but exacerbated the 2014 drought (Keppeler et al., 2024). All told, given the mixed results observed in the literature, it may come to no surprise that SDI variability did not show an interactive effect with dry years on RRs.

Deeper soils showed no difference in RRs between dry and normal years as compared to shallow and mid-depth soils, which were significantly different between dry and normal precipitation years (Figure 22). This would indicate that deeper soils provide a greater resilience to RRs during a drought. Saft et al. (2016) found a similar result where mean solum thickness of a watershed was among the most influential watershed characteristics on changes in the rainfall-runoff relationship during a major drought in Australia. These results contrast with the results of the time series analysis, which indicated that past precipitation was only a significant predictor of streamflow up to three months. Future research should investigate precipitation partitioning into soil-water storage and streamflow production to draw a clear line between definitions of watershed storage and watershed memory.

7. CONCLUSION

The rainfall-runoff relationship of twelve sub-watersheds in the Caspar Creek Experimental Watersheds were examined over seventeen years to assess the effects of past precipitation and watershed characteristics. The sub-watersheds were found to all have a relatively short watershed memory of three months. Of the watershed characteristics tested, aspect, stand density index, and soil depth were found to have significant correlations with annual runoff ratios. Runoff ratios in dry years were significantly different from the rest of the study period. Aspect and soil depth showed clear interactive effects with dry years, demonstrating that north-facing sub-watersheds and deeper soils provided a degree of resilience in runoff ratios in dry years.

From the perspective of an experimental watershed, these results illustrate that the sub-watersheds of the CCEW make relatively convenient replicates, as antecedent precipitation does not appear to be a factor when examining the causes of variation in annual and seasonal streamflow. In effect, each year and season can be treated as independent from the previous, allowing for more powerful statistical analyses of experimental treatments. Since the list of watershed characteristics that influence runoff ratios is fairly short, these can easily be accounted for in future experimental designs.

However, from the perspective of ecological and human communities which depend on the surface water, these results are more mixed. These headwaters show a great ability to quickly recover from a drought year, which may inform best practices for land managers and water users on planning for the possibility of drought. On the other hand, this also means that a wet year provides no measurable hydrological buffer to the onset of a meteorological drought. Some resilience may be provided by watershed characteristics, such as more northly facing slopes and deeper soils, while the benefits of timber harvest on water yield should be balanced with the risk of greater variability. Overall, these results demonstrate a system with little resilience, but high resistance. As a changing climate leads to greater uncertainties in precipitation, we must continue to monitor and steward these small, headwater catchments.

REFERENCES

Abdelnour, A., Stieglitz, M., Pan, F., Mckane, R., 2011. Catchment hydrological responses to forest harvest amount and spatial pattern. Water Resour. Res. 47, 1–18. https://doi.org/10.1029/2010WR010165

Akaike, H., 1974. A new look at the statistical model identification. IEEE Trans. Automat. Contr. 19, 716–723. https://doi.org/10.1109/TAC.1974.1100705

Ambrose, A.R., Baxter, W.L., Wong, C.S., Næsborg, R.R., Williams, C.B., Dawson, T.E., 2015. Contrasting drought-response strategies in California redwoods. Tree Physiol. 35, 453–469. https://doi.org/10.1093/treephys/tpv016

Asarian, J.E., Walker, J.D., 2016. Long-Term Trends in Streamflow and Precipitation in Northwest California and Southwest Oregon, 1953-2012. J. Am. Water Resour. Assoc. 52, 241–261. https://doi.org/10.1111/1752-1688.12381

Aulenbach, B.T., Peters, N.E., 2018. Quantifying Climate-Related Interactions in Shallow and Deep Storage and Evapotranspiration in a Forested, Seasonally Water-Limited Watershed in the Southeastern United States. Water Resour. Res. 54, 3037–3061. https://doi.org/10.1002/2017WR020964

Bachmair, S., Weiler, M., 2012. Hillslope characteristics as controls of subsurface flow variability. Hydrol. Earth Syst. Sci. 16, 3699–3715. https://doi.org/10.5194/hess-16-3699-2012

Baguskas, S.A., Still, C.J., Fischer, D.T., D'Antonio, C.M., King, J.Y., 2016. Coastal fog during summer drought improves the water status of sapling trees more than adult trees in a California pine forest. Oecologia 181, 137–148. https://doi.org/10.1007/s00442-016-3556-y

Bartolini, S., Massai, R., Iacona, C., Guerriero, R., Viti, R., 2019. Forty-year investigations on apricot blooming: Evidences of climate change effects. Sci. Hortic. (Amsterdam). 244, 399–405. https://doi.org/10.1016/j.scienta.2018.09.070

Beven, K.J., Kirkby, M.J., 1979. A physically based, variable contributing area model of basin hydrology. Hydrol. Sci. Bull. 24, 43–69. https://doi.org/10.1080/02626667909491834

Bogan, M.T., Leidy, R.A., Neuhaus, L., Hernandez, C.J., Carlson, S.M., 2019. Biodiversity value of remnant pools in an intermittent stream during the great California drought. Aquat. Conserv. Mar. Freshw. Ecosyst. 29, 976–989. https://doi.org/10.1002/aqc.3109

Brown, A.E., Zhang, L., McMahon, T.A., Western, A.W., Vertessy, R.A., 2005. A review of paired catchment studies for determining changes in water yield resulting from alterations in vegetation. J. Hydrol. 310, 28–61. https://doi.org/10.1016/j.jhydrol.2004.12.010

Cafferata, P.H., Reid, L.M., 2013. Applications of Long-Term Watershed Research To Forest Management in California : 50 Years of Learning from the Caspar Creek Experimental Watersheds. Sacramento, CA.

CAL FIRE, 2016. JDSF South Fork Caspar Timber Harvesting Plan. Fort Bragg, CA.

Calow, R., Robins, N., Macdonald, A., Nicol, A., Orpen, W.R.G., 1999. Planning for groundwater drought in Africa, in: Proceedings of the International Conference on

Integrated Drought Management: Lessons for Sub-Saharan Africa. IHP-V, Technical Documents in Hydrology. pp. 255–270.
Carr, A.E., Loague, K., Vanderkwaak, J.E., 2014. Hydrologic-response simulations for the North Fork of Caspar Creek: second-growth, clear-cut, new-growth, and cumulative watershed effect scenarios. Hydrol. Process. 28, 1476–1494. https://doi.org/10.1002/hyp.9697
Chang, H., Johnson, G., Hinkley, T., Jung, I.W., 2014. Spatial analysis of annual runoff ratios and their variability across the contiguous U.S. J. Hydrol. 511, 387–402. https://doi.org/10.1016/j.jhydrol.2014.01.066
Chang, T.J., Teoh, C.B., 1995. USE OF THE KRIGING METHOD FOR STUDYING CHARACTERISTICS OF GROUND WATER DROUGHTS 1. J. Am. Water Resour. Assoc. 31, 1001–1007.
Chiang, F., Mazdiyasni, O., AghaKouchak, A., 2021. Evidence of anthropogenic impacts on global drought frequency, duration, and intensity. Nat. Commun. 12, 1–10. https://doi.org/10.1038/s41467-021-22314-w
Chung, M., Dufour, A., Pluche, R., Thompson, S., 2017. How much does dry-season fog matter? Quantifying fog contributions to water balance in a coastal California watershed. Hydrol. Process. 31, 3948–3961. https://doi.org/10.1002/hyp.11312
Coble, A.A., Barnard, H., Du, E., Johnson, S., Jones, J., Keppeler, E., Kwon, H., Link, T.E., Penaluna, B.E., Reiter, M., River, M., Puettmann, K., Wagenbrenner, J., 2020. Long-term hydrological response to forest harvest during seasonal low flow: Potential implications for current forest practices. Sci. Total Environ. 730, 138926. https://doi.org/10.1016/j.scitotenv.2020.138926
Creed, I.F., Jones, J.A., Archer, E., Claassen, M., Ellison, D., McNulty, S.G., van Noordwijk, M., Vira, B., Wei, X., Bishop, K., Blanco, J.A., Gush, M., Gyawali, D., Jobbágy, E., Lara, A., Little, C., Martin-Ortega, J., Mukherji, A., Murdiyarso, D., Pol, P.O., Sullivan, C.A., Xu, J., 2019. Managing Forests for Both Downstream and Downwind Water. Front. For. Glob. Chang. 2, 1–8. https://doi.org/10.3389/ffgc.2019.00064
Creed, I.F., Spargo, A.T., Jones, J.A., Buttle, J.M., Adams, M.B., Beall, F.D., Booth, E.G., Campbell, J.L., Clow, D., Elder, K., Green, M.B., Grimm, N.B., Miniat, C., Ramlal, P., Saha, A., Sebestyen, S., Spittlehouse, D., Sterling, S., Williams, M.W., Winkler, R., Yao, H., 2014. Changing forest water yields in response to climate warming: Results from long-term experimental watershed sites across North America. Glob. Chang. Biol. 20, 3191–3208. https://doi.org/10.1111/gcb.12615
de Mendiburu, F., 2021. agricolae: Statistical Procedures for Agricultural Research.
Deitch, M.J., Van Docto, M., Obedzinski, M., Nossaman, S.P., Bartshire, A., 2018. Impact of multi-annual drought on streamflow and habitat in coastal California salmonid streams. Hydrol. Sci. J. 63, 1219–1235. https://doi.org/10.1080/02626667.2018.1492722
Desta, F., Colbert, J.J., Rentch, J.S., Gottschalk, K.W., 2004. Aspect induced differences in vegetation, soil, and microclimatic characteristics of an Appalachian watershed. Castanea 69, 92–108. https://doi.org/10.2179/0008-7475(2004)069<0092:AIDIVS>2.0.CO;2

Dong, C., MacDonald, G.M., Willis, K., Gillespie, T.W., Okin, G.S., Williams, A.P., 2019. Vegetation Responses to 2012–2016 Drought in Northern and Southern California. Geophys. Res. Lett. 46, 3810–3821. https://doi.org/10.1029/2019GL082137

Dracup, J.A., Lee, K.S., Paulson, E.G., 1980. On the statistical characteristics of drought events. Water Resour. Res. 16, 289–296. https://doi.org/10.1029/WR016i002p00289

Dymond, S.F., Richardson, P.W., Webb, L.A., Keppeler, E.T., Arismendi, I., Bladon, K.D., Cafferata, P.H., Dahlke, H.E., Longstreth, D.L. 7, Brand, P.K., Ode, P.R., Surfleet, C.G., Wagenbrenner, J.W., 2021a. A Field-Based Experiment on the Influence of Stand Density Reduction on Watershed Processes at the Caspar Creek Experimental Watersheds in Northern California.

Dymond, S.F., Wagenbrenner, J.W., Keppeler, E.T., Bladon, K.D., 2021b. Dynamic Hillslope Soil Moisture in a Mediterranean Montane Watershed. Water Resour. Res. 57, 1–22. https://doi.org/10.1029/2020WR029170

Flint, A.L., Flint, L.E., Stern, M.A., Ackerly, D.D., Boynton, R., Thorne, J.H., 2024. Characterizing Soil and Bedrock Water Use of Native California Vegetation. Hydrology 11. https://doi.org/10.3390/hydrology11120211

Flint, L.E., Flint, A.L., Mendoza, J., Kalansky, J., Ralph, F.M., 2018. Characterizing drought in California: new drought indices and scenario-testing in support of resource management. Ecol. Process. 7, 1–13. https://doi.org/10.1186/s13717-017-0112-6

Ford, C.R., Laseter, S.H., Swank, W.T., Vose, J.M., 2011. Can forest management be used to sustain water-based ecosystem services in the face of climate change? Ecol. Appl. 21, 2049–2067. https://doi.org/10.1890/10-2246.1

Frahm, G., Junker, M., Schmidt, R., 2005. Estimating the tail-dependence coefficient: Properties and pitfalls. Insur. Math. Econ. 37, 80–100. https://doi.org/10.1016/j.insmatheco.2005.05.008

Gerten, D., Lucht, W., Schaphoff, S., Cramer, W., Hickler, T., Wagner, W., 2005. Hydrologic resilience of the terrestrial biosphere. Geophys. Res. Lett. 32, 1–4. https://doi.org/10.1029/2005GL024247

Goeking, S.A., Tarboton, D.G., 2020. Forests and water yield: A synthesis of disturbance effects on streamflow and snowpack in Western coniferous forests. J. For. 118, 172–192. https://doi.org/10.1093/jofore/fvz069

Guttman, N.B., 1999. Accepting the Standardized Precipitation Index: A Calculation Algorithm. JAWRA J. Am. Water Resour. Assoc. 35, 311–322. https://doi.org/https://doi.org/10.1111/j.1752-1688.1999.tb03592.x

Hahm, W.J., Rempe, D.M., Dralle, D.N., Dawson, T.E., Lovill, S.M., Bryk, A.B., Bish, D.L., Schieber, J., Dietrich, W.E., 2019. Lithologically Controlled Subsurface Critical Zone Thickness and Water Storage Capacity Determine Regional Plant Community Composition. Water Resour. Res. 55, 3028–3055. https://doi.org/10.1029/2018WR023760

Hammerschmidt, S., 2020. Understory Transpiration Rates Following Stand Density Reduction in a Coast Redwood Forest. Universty of Minnesota.

Hao, Z., Singh, V.P., 2016. Review of dependence modeling in hydrology and water resources. Prog. Phys. Geogr. 40, 549–578. https://doi.org/10.1177/0309133316632460

Härdie, W., Lütkepohl, H., Chen, R., 1997. A review of nonparametric time series analysis. Int. Stat. Rev. 65, 49–72. https://doi.org/10.1111/j.1751-5823.1997.tb00367.x

Heddinghaus, T.R., Sabol, P., 1991. A review of the Palmer Drought Severity Index and where do we go from here, in: Proc. 7th Conf. on Applied Climatology. pp. 242–246.

Heim Jr, R.R., 2002. A review of twentieth-century drought indices used in the United States. Bull. Am. Meteorol. Soc. 83, 1149–1166.

Hewlett, J.D., Hibbert, A.R., 1967. Factors affecting the response of small watersheds to precipitation in humid areas. For. Hydrol. https://doi.org/10.1177/0309133309338118

Hewlett, J.D., Hibbert, A.R., 1963. Moisture and Energy Conditions within a Sloping Soil Mass during Drainage. J. Geophys. Res. 68, 1081–1087.

Holland, P.G., Steyn, D.G., 1975. Vegetational Responses to Latitudinal Variations in Slope Angle and Aspect. J. Biogeogr. 2, 179. https://doi.org/10.2307/3037989

Jassal, R.S., Black, T.A., Spittlehouse, D.L., Brümmer, C., Nesic, Z., 2009. Evapotranspiration and water use efficiency in different-aged Pacific Northwest Douglas-fir stands. Agric. For. Meteorol. 149, 1168–1178. https://doi.org/10.1016/j.agrformet.2009.02.004

Jones, J., Ellison, D., Ferraz, S., Lara, A., Wei, X., Zhang, Z., 2022. Forest restoration and hydrology. For. Ecol. Manage. 520, 120342. https://doi.org/10.1016/j.foreco.2022.120342

Jones, J.A., Creed, I.F., Hatcher, K.L., Warren, R.J., Adams, M.B., Benson, M.H., Boose, E., Brown, W.A., Campbell, J.L., Covich, A., Clow, D.W., Dahm, C.N., Elder, K., Ford, C.R., Grimm, N.B., Henshaw, D.L., Larson, K.L., Miles, E.S., Miles, K.M., Sebestyen, S.D., Spargo, A.T., Stone, A.B., Vose, J.M., Williams, M.W., 2012. Ecosystem processes and human influences regulate streamflow response to climate change at long-term ecological research sites. Bioscience 62, 390–404. https://doi.org/10.1525/bio.2012.62.4.10

Jones, J.A., Post, D.A., 2004. Seasonal and successional streamflow response to forest cutting and regrowth in the northwest and eastern United States. Water Resour. Res. 40, 1–19. https://doi.org/10.1029/2003WR002952

Jones, J.A., Swanson, F.J., 2001. Hydrologic inferences from comparisons among small basin experiments. Hydrol. Process. 15, 2363–2366. https://doi.org/10.1002/hyp.474

Kelson, S.J., Carlson, S.M., 2019. Do precipitation extremes drive growth and migration timing of a Pacific salmonid fish in Mediterranean-climate streams? Ecosphere 10. https://doi.org/10.1002/ecs2.2618

Keppeler, E., Lewis, J., 1998. Understanding the Hydrologic Consequences of Timber-harvest and Roading : Four Decades of Streamflow and Sediment Results from the Caspar Creek Experimental Watersheds. North.

Keppeler, E., Lewis, J., Lisle, T., 2003. Effects of Forest Management on Streamflow, Sediment Yield, and Erosion, Caspar Creek Experimental Watersheds, in: Renard,

K.G., McElroy, S.A.., Gburek, W.J., Canfield, H.E., Scott, R.L. (Eds.), First Interagency Conference on Research in the Watersheds. U.S. Department of Agriculture, Agricultural Research Service, Benson, AZ, pp. 77–82.
Keppeler, E., Wagenbrenner, J., Dymond, S., Dralle, D., 2024. Streamflow response to drought in a managed coast redwood catchment. J. Am. Water Resour. Assoc. 1–25. https://doi.org/10.1111/1752-1688.13211
Keppeler, E.T., 1998. The Summer Flow and Water Yield Response to Timber Harvest. Proc. Conf. Coast. Watersheds Caspar Creek Story. PSW-GTR-168. USDA For. Serv. Albany, CA. 35–43.
Keppeler, E.T., Brown, D., 1998. Subsurface drainage processes and management impacts. Ziemer, R.R. (Technical Coord. Proc. Conf. Coast. Watersheds Caspar Creek Story, Gen. Tech. Rep. PSW GTR-168, U.S. For. Serv. Pacific Southwest Res. Station. Albany, CA. 25–34.
Keppeler, E.T., Reid, L., Lisle, T., 2008. Long-term Patterns of Hydrologic Response after Logging in a Coastal Redwood Forest, in: The Third Interagency Conference on Research in the Watersheds. pp. 265–271.
Kerhoulas, L., Polda, W., Kerhoulas, N., Berrill, J.-P., 2020. Physiology and Growth of Douglas-Fir and Redwood Seedlings Planted After Partial Harvesting. Front. For. Glob. Chang. 3, 1–10. https://doi.org/10.3389/ffgc.2020.00049
Keyantash, J., Dracup, J.A., 2002. The Quantification of Drought: An Evaluation of Drought Indices. Am. Meteorol. Soc. 83, 1167–1180.
Kogan, F.N., 1997. Global drought watch from space. Bull. Am. Meteorol. Soc. 78, 621–636.
Kwon, H., Law, B.E., Thomas, C.K., Johnson, B.G., 2018. The influence of hydrological variability on inherent water use efficiency in forests of contrasting composition, age, and precipitation regimes in the Pacific Northwest. Agric. For. Meteorol. 249, 488–500. https://doi.org/10.1016/j.agrformet.2017.08.006
Lechuga, V., Carraro, V., Viñegla, B., Carreira, J.A., Linares, J.C., 2017. Managing drought-sensitive forests under global change. Low competition enhances long-term growth and water uptake in Abies pinsapo. For. Ecol. Manage. 406, 72–82. https://doi.org/10.1016/j.foreco.2017.10.017
Li, Z., Ding, Q., 2024. A global poleward shift of atmospheric rivers. Sci. Adv. 10, eadq0604. https://doi.org/10.1126/sciadv.adq0604
Loritz, R., Kleidon, A., Jackisch, C., Westhoff, M., Ehret, U., Gupta, H., Zehe, E., 2019. A topographic index explaining hydrological similarity by accounting for the joint controls of runoff formation. Hydrol. Earth Syst. Sci. 23, 3807–3821. https://doi.org/10.5194/hess-23-3807-2019
Lukovic, J., Chiang, J.C.H., Blagojevic, D., Sekelic, A., 2021. A Later Onset of the Rainy Season in California. Geophys. Res. Lett. 48.
Lund, J., Medellin-Azuara, J., Durand, J., Stone, K., 2018. Lessons from California's 2012–2016 Drought. J. Water Resour. Plan. Manag. 144, 1–13. https://doi.org/10.1061/(asce)wr.1943-5452.0000984
Luo, L., Apps, D., Arcand, S., Xu, H., Pan, M., Hoerling, M., 2017. Contribution of temperature and precipitation anomalies to the California drought during 2012–

2015. Geophys. Res. Lett. 44, 3184–3192. https://doi.org/10.1002/2016GL072027
McCabe, G.J., Wolock, D.M., 2016. Variability and Trends in Runoff Efficiency in the Conterminous United States. J. Am. Water Resour. Assoc. 52, 1046–1055. https://doi.org/10.1111/1752-1688.12431
McCormick, E.L., Dralle, D.N., Hahm, W.J., Tune, A.K., Schmidt, L.M., Chadwick, K.D., Rempe, D.M., 2021. Widespread woody plant use of water stored in bedrock. Nature 597, 225–229. https://doi.org/10.1038/s41586-021-03761-3
McDonnell, J.J., Evaristo, J., Bladon, K.D., Buttle, J., Creed, I.F., Dymond, S.F., Grant, G., Iroume, A., Jackson, C.R., Jones, J.A., Maness, T., McGuire, K.J., Scott, D.F., Segura, C., Sidle, R.C., Tague, C., 2018. Water sustainability and watershed storage. Nat. Sustain. 1, 378–379. https://doi.org/10.1038/s41893-018-0099-8
McGuire, K.J., Klaus, J., Jackson, C.R., 2024. Interflow, subsurface stormflow and throughflow: A synthesis of field work and modelling. Hydrol. Process. 38, 1–16. https://doi.org/10.1002/hyp.15263
McKee, T.B., Doesken, N.J., Kleist, J., 1993. The Relationshipof Drought Frequency and Duration to Time Scales, in: Eighth Conference on Applied Climatology1. American Meteorological Soceity, Anaheim, California. https://doi.org/10.1002/jso.23002
Merz, R., Blöschl, G., 2009. A regional analysis of event runoff coefficients with respect to climate and catchment characteristics in Austria. Water Resour. Res. 45, 1–19. https://doi.org/10.1029/2008WR007163
Mishra, A.K., Singh, V.P., 2010. A review of drought concepts. J. Hydrol. 391, 202–216. https://doi.org/10.1016/j.jhydrol.2010.07.012
Moges, E., Ruddelll, B.L., Zhang, L., Driscoll, J.M., Larsen, L.G., 2022. Strength and Memory of Precipitation's Control Over Streamflow Across the Conterminous United States Water Resources Research. Water Resour. Res. 58, 1–20. https://doi.org/10.1029/2021WR030186
Nippgen, F., McGlynn, B.L., Emanuel, R.E., Vose, J.M., 2016. Water memory at the Coweeta Hydrologic Laboratory: The effect of past precipitation and storage on hydrologic response. Water Resour. Res. 52, 1–23. https://doi.org/10.1111/j.1752-1688.1969.tb04897.x
NRCS, 2002. Soil survey of Mendocino County, California, Western Part, Natural Resources Conservation Service.
O'Hara, K.L., Cox, L.E., Nikolaeva, S., Bauer, J.J., Hedges, R., 2017. Regeneration Dynamics of coast redwood, a sprouting conifer species: A review with implications for management and restoration. Forests 8, 1–19. https://doi.org/10.3390/f8050144
Perry, T.D., Jones, J.A., 2016. Summer streamflow deficits from regenerating Douglas-fir forest in the Pacific Northwest, USA. Ecohydrology 10, 1–13. https://doi.org/10.1002/eco.1790
Petreshen, J., 2021. Fog Presence and Ecosystem Responses in a Managed Coast Redwood Forest. University of Minnesota.
Petreshen, J., Dymond, S.F., Keppeler, E.T., Allen, S.T., Wagenbrenner, J.W., 2025. Fog presence and ecosystem responses in a managed coast redwood forest. Agric. For. Meteorol. 368, 110525. https://doi.org/10.1016/j.agrformet.2025.110525
Ponce Campos, G.E., Moran, M.S., Huete, A., Zhang, Y., Bresloff, C., Huxman, T.E.,

Eamus, D., Bosch, D.D., Buda, A.R., Gunter, S.A., Heartsill-Scalley, T., Kitchen, S.G., Mcclaran, M.P., Mcnab, W.H., Montoya, D.S., Morgan, J.A., Peters, D.P.C., Sadler, E.J., Seyfried, M.S., Starks, P.J., 2013. Ecosystem resilience despite large-scale altered hydroclimatic conditions. Nature 494, 349–352. https://doi.org/10.1038/nature11836

PRISM Climate Group, 2017. No Title [WWW Document]. Oregon State Univ. URL https://prism.oregonstate.edu (accessed 1.23.21).

R Core Team, 2021. R: A Language and Environment for Statistical Computing.

Rahman, M.A., Yunsheng, L., Sultana, N., 2017. Analysis and prediction of rainfall trends over Bangladesh using Mann–Kendall, Spearman's rho tests and ARIMA model. Meteorol. Atmos. Phys. 129, 409–424. https://doi.org/10.1007/s00703-016-0479-4

Reid, L.M., Lewis, J., 2009. Rates, timing, and mechanisms of rainfall interception loss in a coastal redwood forest. J. Hydrol. 375, 459–470. https://doi.org/10.1016/j.jhydrol.2009.06.048

Reineke, L.H., 1933. Perfecting a stand density index for even-aged forests. J. Agric. Res. 46, 627–638.

Rice, R.M., Tiley, F.B., Datzman, P.A., 1979. A watershed's response to logging and roads: South Fork of Caspar Creek, California, 1967-1976. US For. Serv. Res. Pap. 1967–1976.

Rice, R.M., Ziemer, R.R., Lewis, J., 2004. Evaluating Forest Management Effects On Erosion, Sediment, And Runoff: Caspar Creek And Northwestern California, in: Ice, G.G., Stednick, J.D. (Eds.), A Century of Forest and Wildland Watershed Lessons. Society of American Foresters, Bethesda, Maryland, pp. 223–238.

Richardson, P.W., Seehafer, J.E., Keppeler, E.T., Sutherland, D.G., Wagenbrenner, J.W., 2022. Caspar Creek Experimental Watersheds Phase 2 (1985-2017). 3rd Edition. For. Serv. Res. Data Arch. https://doi.org/https://doi.org/10.2737/RDS-2020-0018-3

Richardson, P.W., Seehafer, J.E., Keppeler, E.T., Sutherland, D.G., Wagenbrenner, J.W., Bladon, K.D., Dymond, S.F., Cole, R.P., 2021. Fifty-eight years and counting of watershed science at the Caspar Creek Experimental Watersheds in northern California. Hydrol. Process. 35, 1–6. https://doi.org/10.1002/hyp.14207

Robeson, S.M., 2015. Revisiting the recent California drought as an extreme value. Geophys. Res. Lett. 42, 6771–6779. https://doi.org/10.1002/2015GL064593

Rodriguez-Iturbe, I., D'Odorico, P., Laio, F., Ridolfi, L., Tamea, S., 2007. Challenges in humid land ecohydrology: Interactions of water table and unsaturated zone with climate, soil, and vegetation. Water Resour. Res. https://doi.org/10.1029/2007WR006073

Saft, M., Peel, M.C., Western, A.W., Zhang, L., 2016. Predicting shifts in rainfall-runoff partitioning during multiyear drought: Roles of dry period and catchment characteristics. Water Resour. Res. 52, 9290–9305. https://doi.org/10.1111/j.1752-1688.1969.tb04897.x

Saft, M., Western, A.W., Zhang, L., Peel, M.C., Potter, N.J., 2015. The influence of multiyear drought on the annual rainfall-runoff relationship: An Australian perspective. Water Resour. Res. 51, 2444–2463. https://doi.org/10.1111/j.1752-

1688.1969.tb04897.x
Saksa, P., Safeeq, M., Dymond, S., 2017. Recent patterns in climate, vegetation, and forest water use in California montane watersheds. Forests 8, 1–16. https://doi.org/10.3390/f8080278
Salve, R., Rempe, D.M., Dietrich, W.E., 2012. Rain, rock moisture dynamics, and the rapid response of perched groundwater in weathered, fractured argillite underlying a steep hillslope. Water Resour. Res. 48, 1–25. https://doi.org/10.1029/2012WR012583
Seager, R., Henderson, N., Cane, M.A., Liu, H., Nakamura, J., 2017. Is there a role for human-induced climate change in the precipitation decline that drove the California drought? J. Clim. 30, 10237–10258. https://doi.org/10.1175/JCLI-D-17-0192.1
Seager, R., Hoerling, M., Schubert, S., Wang, H., Lyon, B., Kumar, A., Nakamura, J., Henderson, N., 2015. Causes of the 2011-14 California drought. J. Clim. 28, 6997–7024. https://doi.org/10.1175/JCLI-D-14-00860.1
Segura, C., Bladon, K.D., Hatten, J.A., Jones, J.A., Hale, V.C., Ice, G.G., 2020. Long-term effects of forest harvesting on summer low flow deficits in the Coast Range of Oregon. J. Hydrol. 585, 124749. https://doi.org/10.1016/j.jhydrol.2020.124749
Segura, C., Noone, D., Warren, D., Jones, J.A., Tenny, J., Ganio, L.M., 2019. Climate, Landforms, and Geology Affect Baseflow Sources in a Mountain Catchment. Water Resour. Res. 55, 5238–5254. https://doi.org/10.1029/2018WR023551
Shafer, B.A., Dezman, L.E., 1982. Development of surface water supply index (SWSI) to assess the severity of drought condition in snowpack runoff areas.
Stednick, J.D., 1996. Monitoring the effects of timber harvest on annual water yield. J. Hydrol. 176, 79–95. https://doi.org/10.1016/0022-1694(95)02780-7
Stoffer, D., 2021. astsa: Applied Statistical Time Series Analysis.
Sun, G., Caldwell, P. V., Mcnulty, S.G., 2015. Modelling the potential role of forest thinning in maintaining water supplies under a changing climate across the conterminous United States. Hydrol. Process. 29, 5016–5030. https://doi.org/10.1002/hyp.10469
Swain, D. l., Tsiang, M., Haugen, M., Singh, D., Charland, A., Rajaratnam, B., Diffenbaugh, N. s., 2014. The Extraordinary California Drought of 2013/2014: Character, Context, and the Role of Climate Change. Bull. Am. Meteoroligical Soc. 95, S3–S7.
Swain, D.L., 2021. A shorter, sharper rainy season amplifies California wildfire risk. Geophys. Res. Lett. https://doi.org/10.1029/2021GL092843
Swift Jr, L.W., Cunningham, G.B., Douglass, J.E., 1988. Climatology and hydrology, in: Forest Hydrology and Ecology at Coweeta. Springer, New York, NY, pp. 35–55.
Thornthwaite, C.W., 1948. An Approach toward a Rational Classification of Climate. Geogr. Rev. 38, 55. https://doi.org/10.2307/210739
Tukey, J.W., 1949. Comparing Individual Means in the Analysis of Variance. Biometrics 5, 99–114. https://doi.org/10.2307/3001913
Wagenbrenner, J., 2018. Addendum to Caspar Creek Experimental Watersheds Experiment Three Study Plan: The influence of forest stand density reduction on watershed processes in the South Fork 1–28.

Wang, S.Y.S., Yoon, J.-H., Becker, E., Gillies, R., 2017. California from drought to deluge. Nat. Clim. Chang. 7, 465–468. https://doi.org/10.1038/nclimate3330
Wemple, B.C., Jones, J.A., 2003. Runoff production on forest roads in a steep, mountain catchment. Water Resour. Res. 39. https://doi.org/10.1029/2002WR001744
White, M.A., de Beurs, K.M., Didan, K., Inouye, D.W., Richardson, A.D., Jensen, O.P., O'Keefe, J., Zhang, G., Nemani, R.R., van Leeuwen, W.J.D., Brown, J.F., de Wit, A., Schaepman, M., Lin, X., Dettinger, M., Bailey, A.S., Kimball, J., Schwartz, M.D., Baldocchi, D.D., Lee, J.T., Lauenroth, W.K., 2009. Intercomparison, interpretation, and assessment of spring phenology in North America estimated from remote sensing for 1982-2006. Glob. Chang. Biol. 15, 2335–2359. https://doi.org/10.1111/j.1365-2486.2009.01910.x
Wilhite, D.A., Glantz, M.H., 1985. Understanding the drought phenomenon: The role of definitions. Water Int. 10, 111–120. https://doi.org/10.4324/9780429301735-2
Williams, A.P., Seager, R., Abatzoglou, J.T., Cook, B.I., Smerdon, J.E., Cook, E.R., 2015. Contribution of anthropogenic warming to California drought during 2012–2014. Geophys. Res. Lett. 42, 6819–6828. https://doi.org/10.1002/2015GL064924.Received
World Meteorological Organization, I., 2008. Guide to Meteorological Instruments and Methods of Observation, 7th ed. Geneva, Switzerland.
Yetemen, O., Istanbulluoglu, E., Flores-Cervantes, J.H., Vivoni, E.R., Bras, R.L., 2015. Ecohydrologic role of solar radiation on landscape evolution. Water Resour. Res. 51, 1127–1157. https://doi.org/10.1111/j.1752-1688.1969.tb04897.x
Ziemer, R.R., 1998a. Proceedings of the conference on coastal watersheds: the Caspar Creek story. Ukiah, CA.
Ziemer, R.R., 1998b. Monitoring watersheds and streams, USDA Forest Service General Technical Report.
Ziemer, R.R., 1981. Storm flow response to road building and partial cutting in small streams of northern California. Water Resour. Res. 17, 907–917. https://doi.org/10.1029/WR017i004p00907
Ziemer, R.R., Albright, J.S., 1987. Subsurface pipeflow dynamics of north-coastal California swale systems, in: Erosion and Sedimentation in the Pacific Rim (Proceedings of the Corvallis Symposium, August, 1987). pp. 71–80.
Ziemer, R.R., Lewis, J., Keppeler, E.T., 1996. Hydrologic consequences of logging second-growth redwood watersheds, in: LeBlanc, J. (Ed.), Conference on Coast Redwood Forest Ecology and Management; June 18-20, 1996, Arcata, CA. University of California, Berkeley, CA, pp. 131–133.

APPENDIX A: Drought Definitions

Drought is primarily defined by a significant decrease in precipitation, however the use of several different hydrometeorological variables in the study of drought, as well as socioeconomic impacts, has led to multiple definitions of drought in the literature. These can be classified into four general categories, and each have associated indices.

Meteorological drought, or the significant and temporary reduction in precipitation over a region, is perhaps the most commonly used definition. The standard precipitation index (SPI) is a commonly used metric that can be used on a variety of timescales. The index compares observed precipitation as a departure from a transformed normal distribution based on a long-term record (McKee et al., 1993; Mishra and Singh, 2010). SPI has been found to be useful for understanding soil moisture at short timescales, such as weeks to months, while at longer timescales, it is better correlated to groundwater storage. SPI is more comparable across different geographies and environments than the Palmer drought severity index (PDSI), discussed below. It also benefits from only needing a precipitation record and thus avoids complications of other indices. However, it requires a lengthy precipitation record to construct a robust probability distribution, and thus is not appropriate for smaller datasets and may not be available in all locations. Additionally, it does not account for changes in evapotranspiration, particularly those driven by climate change, leading to the proposal of SPEI as an alternative (Keyantash and Dracup, 2002).

Hydrological drought occurs when there is a significant loss in the quantity of surface and subsurface water resources. This is most widely monitored using streamflow data, as well as lake and reservoir level changes (Dracup et al., 1980; Flint et al., 2018). Surface water supply index (SWSI) uses monthly probability distributions of reservoir storage, streamflow, snowpack, and precipitation, based on historical records (Shafer and Dezman, 1982). It is most commonly applied to monitor drought impacts on human water use, such as municipal water supplies, irrigation, and hydroelectric power generation. The standard runoff index (SRI) is a recently developed index that is conceptually similar to SPI and is often used in conjunction with SPI to understand the progression from meteorological drought to hydrological drought (Saksa et al., 2017).

Additional drought definitions exist including groundwater drought (Calow et al., 1999; Chang and Teoh, 1995), agricultural drought (Aulenbach and Peters, 2018; Heddinghaus and Sabol, 1991; Heim Jr, 2002; Kogan, 1997), and socioeconomic drought (AMS, 2013), each with their own unique indices. Although each has the ability to interact and potentially exacerbate each other, they are beyond the scope of this particular research question.

APPENDIX B: Watershed Properties Influence on Past Precipitation Lag Analysis

When categorized by aspect, the lag correlations between precipitation and streamflow did not show strong differences at any time step between north, south, and west facing sub-watersheds (Figure 23). The lag correlations also did not show any difference at any time step when categorized into high, mid, and low SDI (Figure 24). Soil depth also did not reveal any difference in the lag correlations between precipitation and streamflow (Figure 25).

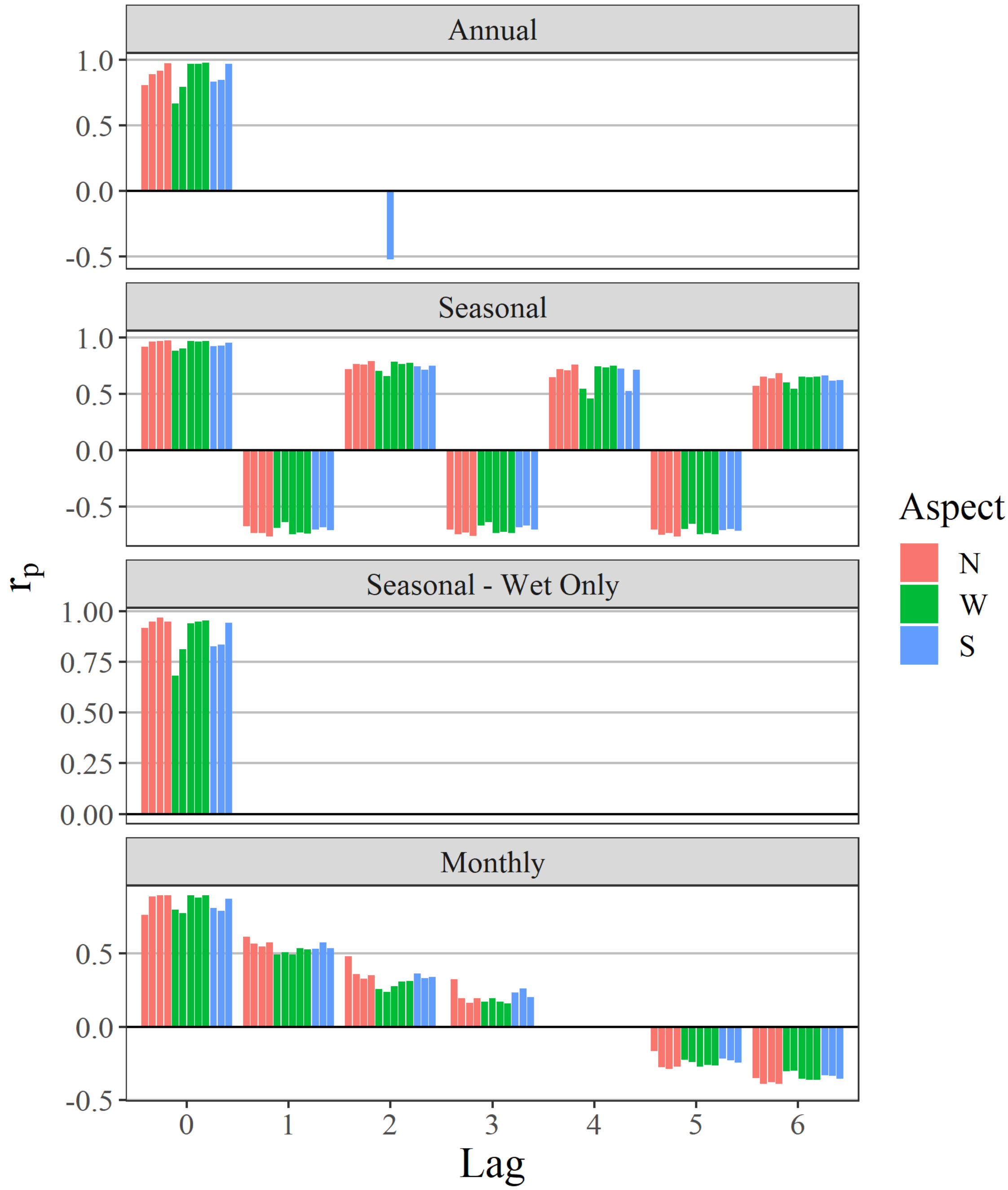

Figure 23. Past precipitation and streamflow lag correlations categorized by aspect.

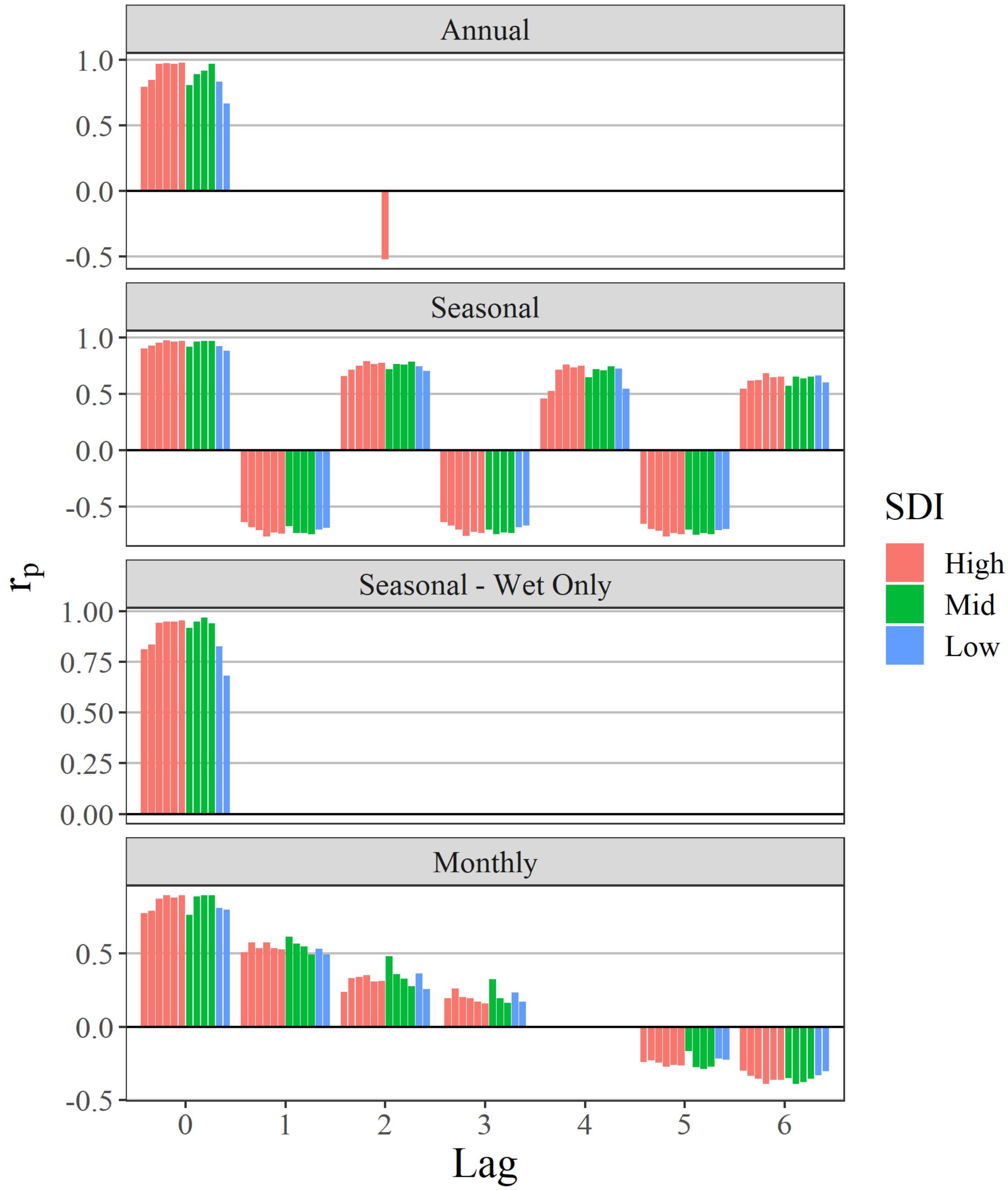

Figure 24. Past precipitation and streamflow lag correlations categorized by SDI.

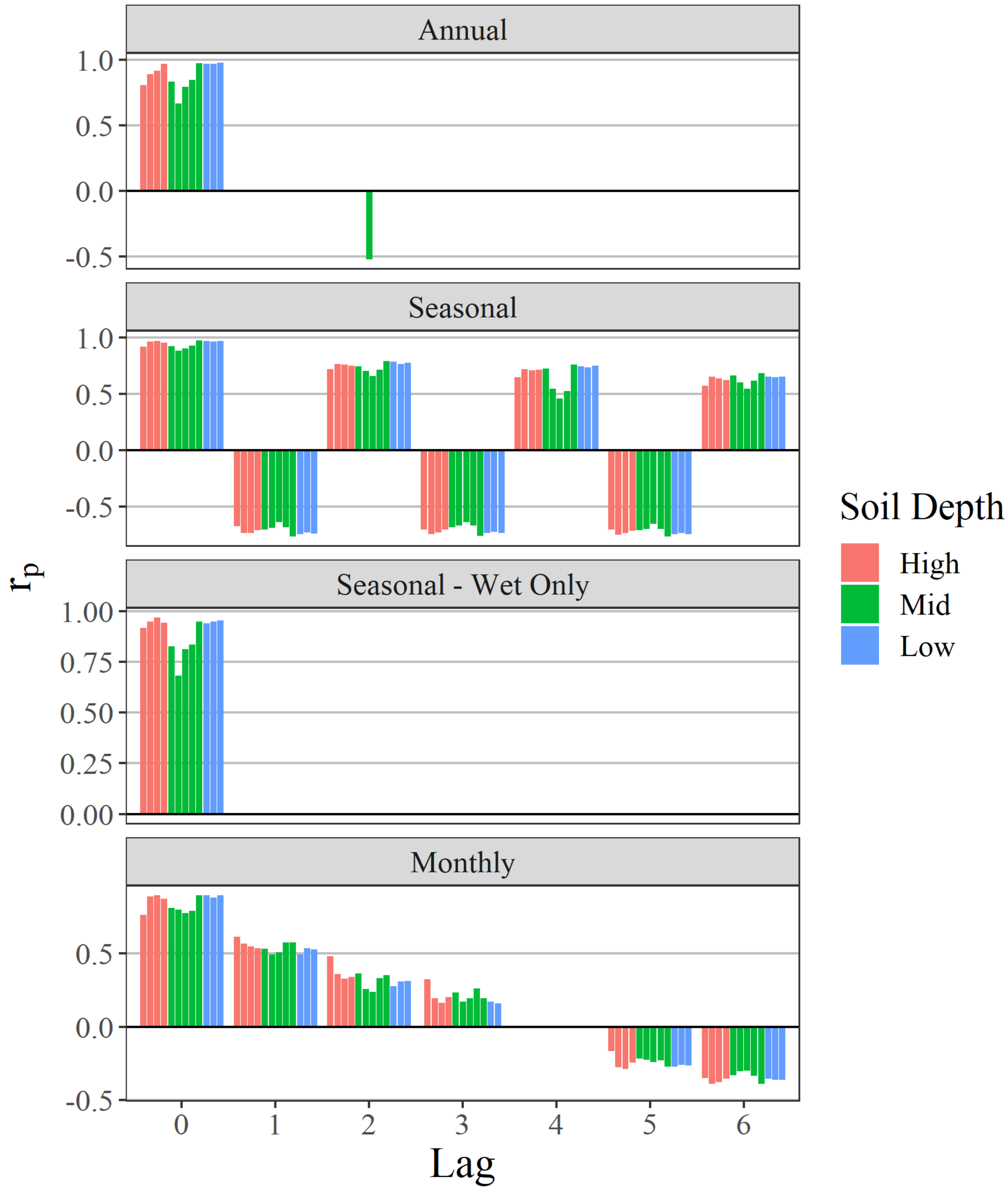

Figure 25. Past precipitation and streamflow lag correlations categorized by soil depth.

The annual lag correlations between precipitation and runoff ratios, when categorized by aspect, showed that sub-watersheds were significant at similar rates across bins (Figure 26). Three of four north facing, four of five west facing, and two of three south facing sub-watersheds had significant lag correlations at the zero step. The west facing sub-watersheds appeared to have relatively stronger correlations than the north or south facing sub-watersheds. At the seasonal timestep, the west bin had the strongest and greatest number of significant lag correlations. At each step, the sub-watersheds which oscillated opposite the majority were both north facing. Relative to the annual timestep, the wet-only seasonal timestep had one more significant north facing sub-watershed and one less significant south facing sub-watershed. The west facing sub-watersheds did not appear to have stronger correlations than the north or south facing sub-watersheds.

When categorized by SDI, high SDI sub-watersheds had consistently stronger correlations relative to mid and low SDI sub-watersheds (Figure 27). Four of six high SDI, three of four mid SDI sub-watersheds, and one of two low SDI sub-watersheds were significant. At the seasonal timestep, the high SDI sub-watersheds showed the most consistent pattern of oscillation. No low SDI sub-watershed had significant correlations in the wet only seasonal timestep, and the high and mid SDI sub-watersheds showed no difference in correlation strength.

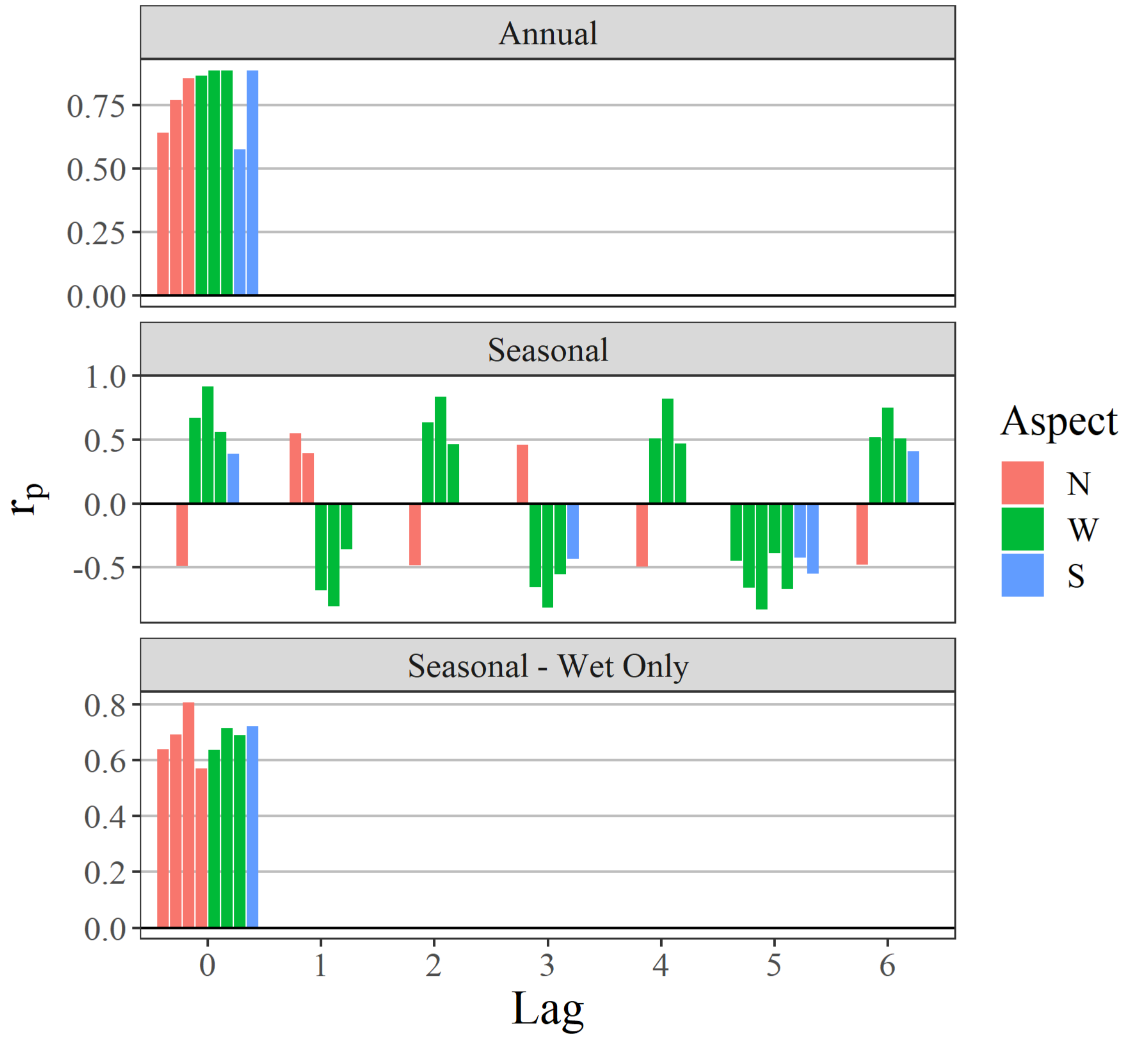

Figure 26. Past precipitation and runoff ratio lag correlations categorized by aspect.

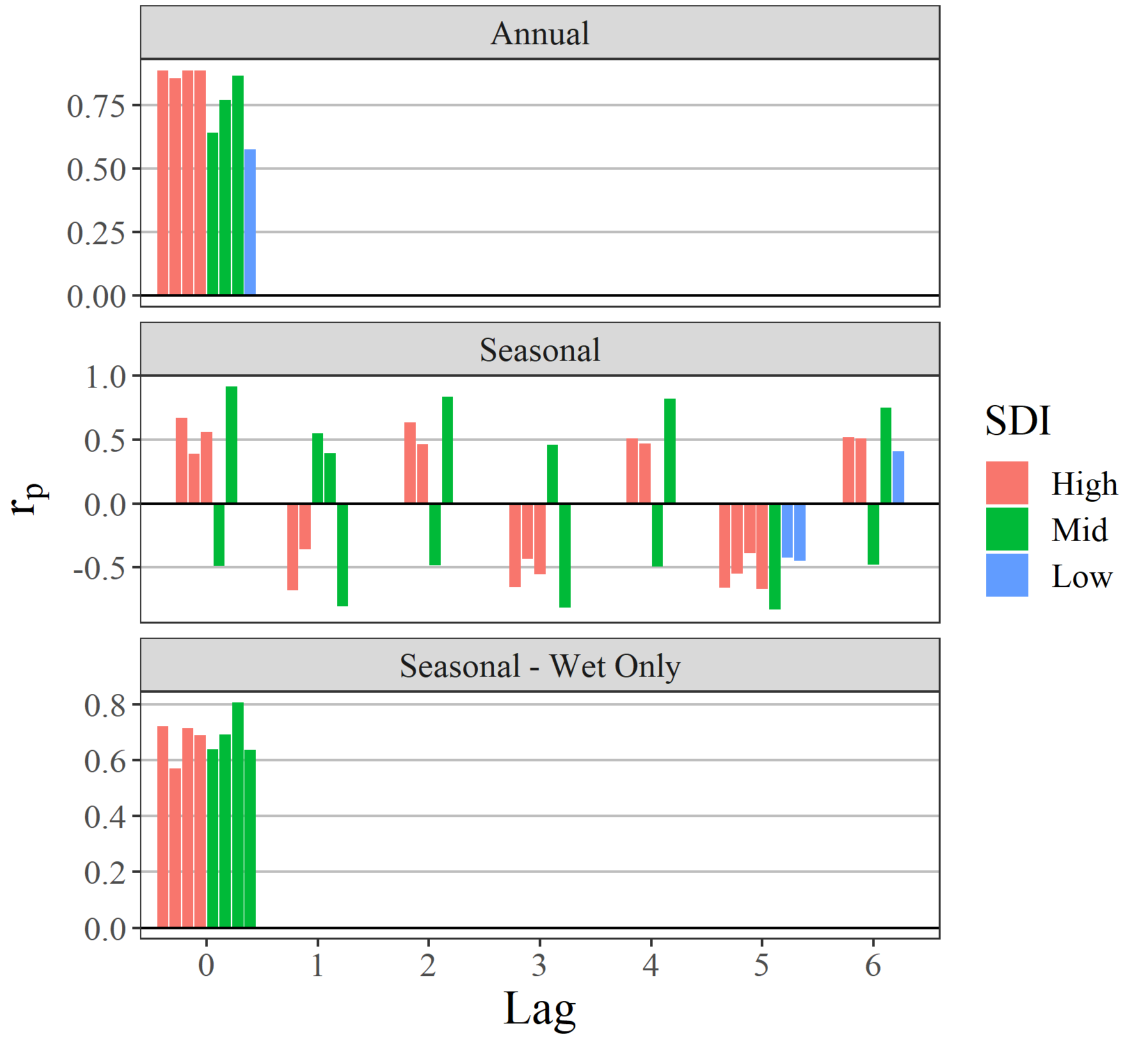

Figure 27. Past precipitation and runoff ratio lag correlations categorized by SDI.

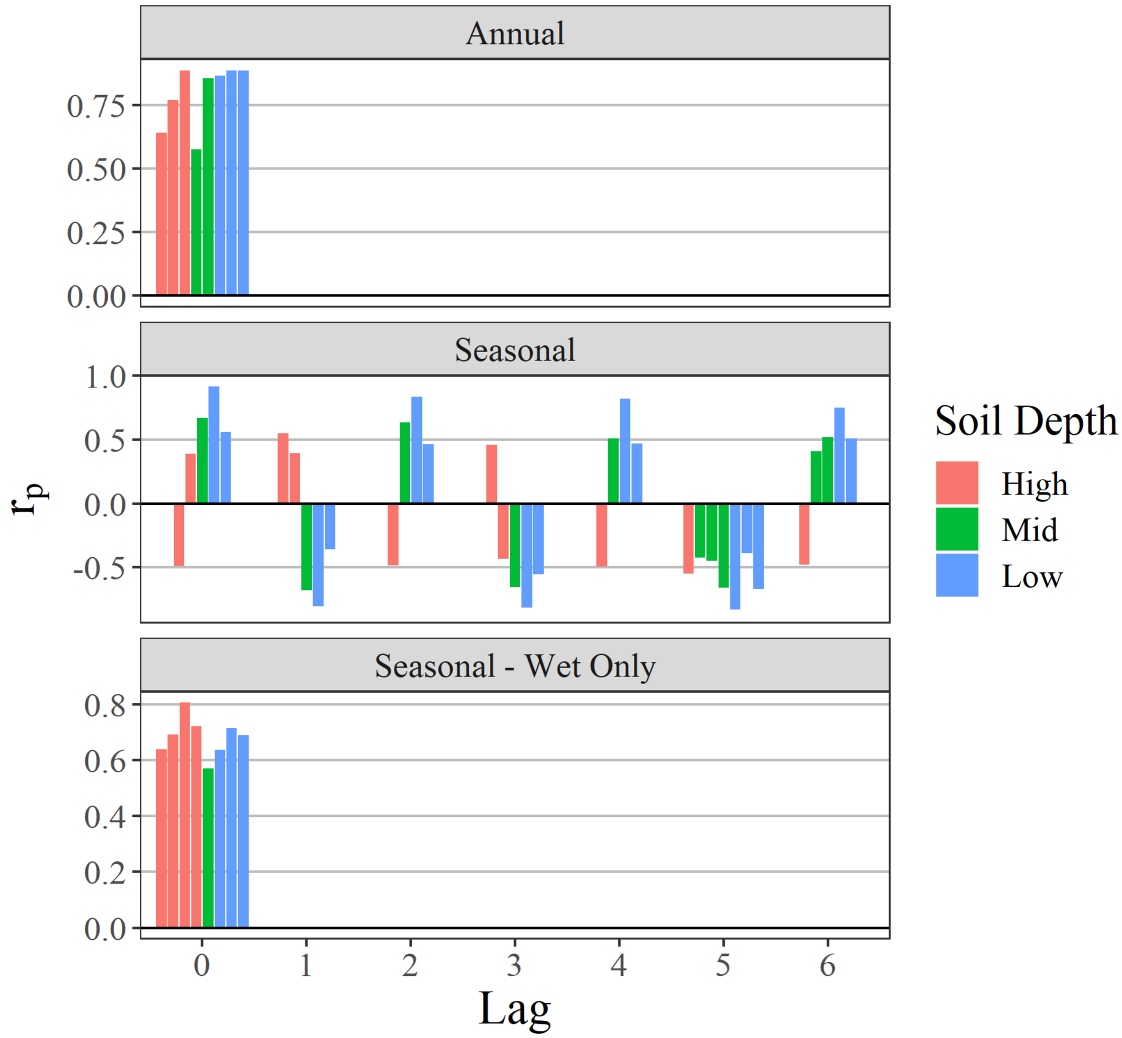

Figure 28. Past precipitation and runoff ratio lag correlations categorized by soil depth.

At the annual timestep, three of four watersheds with deep soils and all three watersheds with shallow soil were significant, however only two of five sub-watersheds with mid-level depth were significant (Figure 28). The shallow soil sub-watersheds had the strongest correlations. At the seasonal timestep, the shallow soil sub-watersheds showed the most consistent oscillation. At the wet seasonal only time step, the deep and mid depth bins each had one less significant sub-watershed relative to the annual timestep. No difference in the correlation strengths among the soil depth categories were found at the wet season only time step.